Dr #1307

MASTER

ORNL/Sub-3988/1

Treatment of Low Strains and Long Hold Times in High Temperature Metal Fatigue by Strainrange Partitioning*

S. S. Manson
Professor, Mechanical and Aerospace Engineering
Case Western Reserve University

Ronald Zab
Graduate Student
Case Western Reserve University

*Final report on research performed under Subcontract No. 3988 as a part of the ORNL High-Temperature Structural Design Program

Prepared by
Mechanical and Aerospace Engineering
Case Western Reserve University

Prepared for
OAK RIDGE NATIONAL LABORATORY
Oak Ridge, Tennessee 37830
operated by
UNION CARBIDE CORPORATION
for the
ENERGY RESEARCH AND DEVELOPMENT ADMINISTRATION

ORNL/Sub-3988/1
Dist. Category UC-79,
-79e, -79h, -79k

TREATMENT OF LOW STRAINS AND LONG HOLD TIMES IN HIGH TEMPERATURE METAL FATIGUE BY STRAINRANGE PARTITIONING *

S. S. Manson
Professor, Mechanical and Aerospace Engineering
Case Western Reserve University

Ronald Zab
Graduate Student
Case Western Reserve University

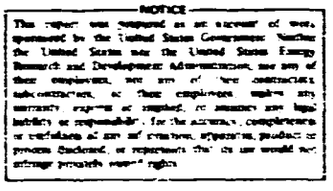

*Final report on research performed under Subcontract No. 3988 as a part of the ORNL High-Temperature Structural Design Program

Date Published: August 1977

Prepared by
Mechanical and Aerospace Engineering
Case Western Reserve University

Prepared for
OAK RIDGE NATIONAL LABORATORY
Oak Ridge, Tennessee 37830
operated by
UNION CARBIDE CORPORATION
for the
ENERGY RESEARCH AND DEVELOPMENT ADMINISTRATION

Contract No. W-7405-eng-26

CONTENTS

INTRODUCTION

For the past 2½ years Case Western Reserve University has been engaged in a study on the possible applications of Strainrange Partitioning (SRP) to the treatment of high temperature creep-fatigue problems. One part of this program has been supported by the Oak Ridge National Laboratory, and is directed at special applications involved in advanced nuclear reactors such as the liquid metal fast breeder reactor. The first phase was the preparation of an Interpretive Report* describing various alternatives for treating creep-fatigue problems, emphasizing Strainrange Partitioning as a method which has merit for this application. While many features of the method were described in this report, and in fact much new progress was made during its preparation, a number of developments were left for future study. As a result of the report a limited follow-on contract was initiated on May 1, 1976 and expired on September 30, 1976. It is the purpose of this report to describe in brief the progress made during the contract period.

The focus of study during this period was the treatment of low strains and long hold periods, since these were major areas requiring further investigation, as identified in the Interpretive Report. We shall, therefore, concentrate here on the progress that has been made on this subject. However, brief discussions will also be presented on other subjects which have only been cursorily studied. These are environmental effects, metallurgical effects, and grain size considerations.

One of the major conclusions reached in the Interpretive Report is that there is an urgent need for developing techniques for treating low strains, particularly when long hold-times are involved. None of the candidate methods for handling creep-fatigue problems can readily address this subject without additional progress beyond that available at the time of the Interpretive Report preparation. Strainrange Partitioning,

*Chapter 4, Ref. 1.

in particular, concentrating as it does on the inelastic strains developed during the service cycle, must therefore be extended before it can be confidently applied to LMFBR components involving low strains. This is especially true when long hold-times are involved because of the transfer of one type of strain to another during the hold period. Since environment can affect both the rheological behavior, as well as the fatigue and fracture behavior, it is clear that the extension of Strainrange Partitioning into the low strain (and) long cycle time regime will involve either:

a) the establishment of accurate constitutive equations in the strain/time/environment regime of interest so that the cyclic strain can be appropriately partitioned into the components characteristically used in the Strainrange Partitioning life relations, or

b) the semi-experimental approach wherein the hysteresis loop for the actual cycle of interest is experimentally determined. While precluding the need for accurate constitutive equations which determine the stresses and total strains involved in the cycle, there still remains the need for practical procedures for partitioning the measured total strains into strain-range components characteristically used in the SRP life relations, or

c) the engineering estimation of some of the required stress or strain quantities, and the computation of the remainder of the quantities using simplified constitutive equations, thereby determining an internally consistent set of stresses and strain components characteristically required in the SRP life relations.

Whichever of the above methods is used, some account must be provided for the environmental effect. This subject can be given only cursory treatment here, but is obviously of great importance in components expected to operate in oxidizing environments at high temperatures for periods up to 30 years or more.

Method (a) above will become viable when the extensive program on development of constitutive equations is completed. If, through these equations, each increment of plasticity, transient creep and steady state creep is determined at each increment of load or time, it then becomes a

simple matter to formulate the pp, cp, pc, and cc strain components that develop for the cycle. Hence there is no problem in applying the SRP life relations, even when the inelastic components are small. Under these conditions the whole problem degenerates to a simple approach directly analogous to the treatment of large strains already developed. For this reason, this approach will not be further discussed here, except to express the hope that the final development will soon be realized so that it can be of direct use in SRP application.

The other two approaches have therefore been followed in this limited program. Examples of results to date will be described in the remainder of this report.

TREATMENT OF LOW STRAINS AND LONG HOLD TIMES

Basis of Analysis

The development of the procedure will be illustrated here by first treating large strain problems for which experimental data are available to check results. We shall illustrate both the semi-experimental procedure, and the approach involving an engineering estimation of the essential features of the hysteresis loop required in the analysis. Then we shall extend the concepts to the treatment of low strains by the same principles. The procedures will be applied to problems involving hold times in tension or in compression, combined tension and compression hold, and continuous cycling at various frequencies. In the initial analysis we shall neglect possible changes in ductility due to exposure. Later in the report such ductility effects will be briefly considered.

Basic Data Required In order to treat creep-fatigue problems by Strain-range Partitioning it is desirable to know a number of properties associated with the material and some informantion associated with the particular problem being treated. Usually the information will be readily available through basic material characterization, but even if not known accurately it may be possible to estimate the required quantitites with reasonable accuracy. In the discussion to follow we shall assume that the required information is available for large as well as small strains; if small strain information is difficult to obtain directly, it will be assumed that the determination

is made by simple linear extrapolation from high strain data. We shall illustrate the procedure in connection with problems of moderately high strainrange because these are the only ones for which good experimental data are available whereby the adequacy of the general procedure may be checked, but there is no problem in extending the procedure for problems of small strain. Thus, we shall show results of calculations involving small strains although there are, of course, no extensive data available to check the validity of these calculations.

Figure 1 shows the ideal type of data base desired for life analysis by this method. In Figure 1(a) are shown the basic life relations for $\Delta\varepsilon_{pp}$, $\Delta\varepsilon_{cc}$, $\Delta\varepsilon_{cp}$, and $\Delta\varepsilon_{pc}$ types of strainranges. They are shown as mildly-temperature dependent functions, although for at least two materials (316 SS and 2¼ Cr - 1 Mo steels) studied (Ref. 2) they were found to be essentially independent of temperature. Also included in this figure is a family of elastic (el) lines, obtained from rapid cycling in association with $\Delta\varepsilon_{pp}$ tests. These lines are temperature-dependent, reflecting the flow strength dependency of the material with temperature.

Figure 1(b) shows the cyclic stress-strain curve, OA, for rapid cycling of the material. There is, of course, an interdependence between OA and the pp and el life lines of Fig. 1(a). For any selected life value, the el line can be used to determine the stress range, and the el and pp lines together can be used to determine the total strain range. Thus the curve OA can be constructed from a knowledge of the life relations. In this approach the implication is that plastic strain is always present, even at very low stresses which appear to lie on the linear (elastic) portion of the curve, but the deviation from linearity is very small. It is advantageous to regard a pp strain to be present at all stress ranges because it enables the determinations of plasticity strains, even though they are small, when treating low total strains. Also shown in Fig. 1(b) is the rapid-cycling hysteresis loop ABCDA for one strain range. This loop can be constructed from the shape of the cyclic stress-strain curve through application of the well known double-amplitude construction principle. That is, CDA can be constructed

from a knowledge of OA by choosing C as the origin and doubling all stress and strain values along OA. Similarly, ABC is symmetrical to CDA. Although only one cyclic stress-strain curve and hysteresis loop is shown in Fig. 1(b), numerous curves could be drawn, one at each strain range. These curves are all quite sensitive to temperature, being a reflection of the rheological dependence on temperature, but once the pp and el lines in Fig. 1(a) are known for a selected temperature any required hysteresis loop in Fig. 1(b) can be constructed.

The third desirable ingredient is shown in Fig. 1(c). It is the relation between stress and secondary (steady state) creep rate in a cyclic creep test (or in any cyclic test involving stopping at specific stress levels and observing the creep rate once it has stabilized). In Ref. 3 it was shown that the relationship between secondary creep rate and stress can be represented by a power law. Thus Fig. 1(c) shows linear plots of creep rates and stress on log-log coordinates. These curves can be expected to be strongly dependent on temperature. For illustrative purposes the lines for different temperatures are shown parallel, but other geometric relations are possible.

The final ingredient of the life analysis is shown in Fig. 1(d). It is a stabilized hysteresis loop for the duty cycle under analysis. The tick marks represent the time sequence at which various points are encountered during the cycle. Although an experimentally determined hysteresis loop is highly desirable, it is not absolutely necessary. In its absence it can be approximated from other specified variables (for example, linear stress ramping as later discussed or other pattern of stress or strain variation). However, it should be emphasized that hysteresis loops stabilize rapidly, and it is necessary to traverse only a small fraction of life expectancy in order to obtain this valuable adjunct to the analysis, or to provide valuable information useful in cross-checking some facets of the analysis.

Outline of Procedure To illustrate the procedure we shall analyze a test reported by Conway et al (Ref. 4) involving strain-hold to long-times (1.0 hrs per cycle). The strainrange for these tests was high (2%), but it will be seen that exactly the same procedure as discussed for this high strain problem can be used to analyze low strain problems. In fact, we shall show results for such calculations after we have described the method.

The ingredients analogous to Fig. 1 applicable to this problem are shown in Fig. 2. Since the test was conducted at a constant temperature of 1200F, only this temperature is reflected in Figs. 2(b,c, and d). Fig. 2(a) shows the strain pattern imposed as the test condition, and Fig. 2(e) is the stress-strain response, showing the relaxation that was measured during the strain-hold period. The time markings on Fig. 2(e) correspond to points selected in Fig. 2(f).

The analysis is shown in Fig. 3. First the secondary creep is calculated in each half of the cycle. Since the compressive half of the cycle involves only rapid loading the creep is negligible; only the tensile half involves creep. Fig. 3(a) shows the creep rates and the integrated area (representing the total creep strain) as .000975. In Fig. 3, item (b), it is also shown that the plastic strainrange is .0160 as deduced from the stress range (elastic strainrange) and the life relationships of Fig. 2(a). The total inelastic strainrange is .0167, as deduced from the width of the hysteresis loop, from which the transient creep strainrange is determined by substracting the plastic strainrange.

It then becomes possible to calculate the strainrange components. As discussed in Ref. 5, the "creep" in each half cycle consists of the secondary creep plus 10% of the transient creep, if identified. Since in this case the transient creep is known, the total tensile creep, item (e), is .001045. Now, since the "creep" in the compressive half of the cycle is zero, there can be no reversed creep; thus $\Delta\varepsilon_{cc} = 0$. All the tensile "creep" is reversed by plasticity; thus $\Delta\varepsilon_{cp} = .001045$. The remainder of the inelastic

strainrange is converted to reversed plasticity $\Delta\varepsilon_{pp}$, and is .015655, according to item (c) of Fig. 3. Thus, this problem involves $\Delta\varepsilon_{cp}$ and $\Delta\varepsilon_{pp}$, and as shown in item (j) and (k) results in a computed life of 155 cycles. This compares to a measured life of 103 cycles, which is a reasonably close correlation. Similar calculations were made for the other two 2% strainrange hold-time tests reported by Conway in Ref. 4. In one the hold-time was 60 min. and the other 30 min. Life predictions were successively 156 and 149 cycles, compared to the experimental values of 117 and 76 respectively.

Alternate Procedure Before presenting the calculations for small strains it is appropriate to describe an alternate procedure for handling the stress relaxation problem just discussed. In the previous discussion it was assumed that the stress pattern during the relaxation is known from experimental observation. Suppose, however, experimental determination is inconvenient, can we still handle the problem? Initially, let us assume that the maximum stress is known from the strainrange and cyclic stress-strain curve. That is, in Fig. 4 we assume that RP follows the cyclic stress-strain curve (by the double-amplitude rule of stress and strain, Fig. 1(b).) Recognizing the large strain amplitude of 2% involved in this problem, we reasonably assume that the stresses at R and P will be approximately equal in magnitude; thus there is no ambiguity as to the coordinates of point R in the initial construction of the hysteresis loop. The stress σ_p at point P will be known in magnitude. The stress pattern PQ'Q can then be determined from a single creep relaxation analysis as follows:

Letting ε_c be the creep strain at any time t after the initiation of hold, and also letting:

ε_e be the relaxed elastic strain at this time and σ be the relaxed value of stress at this time, then, neglecting primary (transient) creep, and considering only the secondary creep rate

$$\dot{\varepsilon}_c = A\sigma^n \text{ or } \frac{d\varepsilon_c}{dt} = A\sigma^n \qquad (1)$$

from the power-law relation shown in Ref. 3 where A and n are material constants dependent on the temperature.

By Hooke's Law $d\varepsilon_e = \frac{d\sigma}{E}$ or $\frac{d\varepsilon_e}{dt} = \frac{1}{E}\frac{d\sigma}{dt}$ (2)

But since strain is held constant $\frac{d\varepsilon_t}{dt} = \frac{d\varepsilon_e}{dt} + \frac{d\varepsilon_c}{dt} = 0$ (3)

Combining (1), (2) and (3) results in $\frac{d\sigma}{\sigma^n} = -AE dt$ (4)

Integrating eq (4),

$$\frac{\sigma_{Q'}^{-n+1}}{-n+1} - \frac{\sigma_p^{-n+1}}{-n+1} = -AE\ [t-0] = -AEt, \tag{5}$$

or,

$$\sigma_{Q'} = \left[\sigma_p^{-n+1} + (n-1)\ AEt\right]^{\frac{1}{-n+1}} \tag{6}$$

After the entire hold-period t_H, the relaxed stress becomes

$$\sigma_Q = \left[\sigma_p^{-n+1} + (n-1)AEt_H\right]^{\frac{1}{-n+1}} \tag{7}$$

For the problem illustrated in Fig. 2, the application of the double-amplitude cyclic stress-strain relation results in a stress σ_p of 41.87 ksi, and since the constants in the creep equation (1) are known from NASA data (Ref. 5) or unpublished data obtained during preparation of Ref. 5

$n = 7.14$ $\qquad A = 2.55 \times 10^{-17}$ (σ in ksi, t in seconds)

$E = 22 \times 10^3$ ksi

Thus $\sigma_Q = \left[\sigma_p^{-6.14} + 3.44 \times 10^{-12} t\right]^{\frac{1}{-6.14}}$ (8)

A plot of stress relaxation according to Eq. (8) is shown in Fig. 5 (a); the agreement is remarkably good considering the basic approximations involved and the fact that the creep rate determinations were made by different investigators and on different lots of material from those involved in the relaxation tests, and that transient creep was omitted. To check the validity of this approach to other tests, additional calculations were made for the two other relaxation tests reported in Ref. 4. The temperature

and strainrange were the same as above, but in one case the hold time was 30 min.; in the other 1 min. The results are shown in Fig. 5(b) and (c). For the 30 min. hold test, the agreement is still very good; for the 1 min. hold the effect of the transient creep is apparent in the early seconds, but after about 30 sec the agreement again becomes excellent.

The next step is to determine how much of each strainrange component type develops during the cycle:

a) The total amount of plastic flow during the tensile half is known from the cyclic stress-strain curve, or as expressed by the linear life relations, shown in Fig. 4(c). Knowing the stress range RP, the elastic strainrange establishes the point M on the elastic life line, from which the point N on the plastic life line vertically above M establishes a plastic strainrange of .0160.

b) The tensile creep is equal to the elastic strain from P to Q (or alternatively, the integrated creep during PQ according to Eq (1) above, which yields exactly the same result.) Thus, in this case the tensile creep strain is .000975.

c) A small amount of ambiguity develops in the determination of the compressive plasticity if determined from consideration of the shape of the curve QR. We cannot construct this reverse piece of the hysteresis loop from the double-amplitude cyclic stress-strain curve alone, starting with Q as an origin. The plastic flow from Q to R based only on the stress range involved would be expected to be too low to balance both the tensile plastic and creep flow. Actually, a more appropriate way to construct the compressive half of the loop is to add the imaginary segment PTQ in Fig. 4(a) so that TQR, in conjunction with the cyclic stress-strain curve yields a compressive plastic flow which is equal to the tensile plastic flow plus the relaxation creep flow. This adds the complication that if $\sigma_T = \sigma_R$ then σ_p is no longer equal to σ_R, which was our original premise. Therefore the problem becomes one of trial and error to determine the appropriate location of the hysteresis loop to establish consistency with the rheological behavior. In general, the rheological behavior, as affected by the cycle itself, influences the individual creep and elasticity components. This is evident in Fig. 5 wherein it is noted that the maximum tensile stress reached depends on the hold-time. The longer the hold time, the lower

the stress. To get exact behavior, the constitutive equations must be better established than they are now. But the approximate answer can readily be determined in this case by stating that the behavior of QR in the vicinity of R is such that the plastic flow developed on compression is equal to the tensile plastic flow plus the tensile creep flow during PQ.

d) Thus, from the above considerations, the $\Delta\varepsilon_{cp}$ deformation is equal to the tensile creep deformation .000975, and the remainder of the inelastic strain in $\Delta\varepsilon_{pp}$, so that $\Delta\varepsilon_{pp} = .0160$.

e) The life is then calculated by the Interaction Damage Rule as

$$f_{pp} = \frac{.01573}{.01670} = .9419 \qquad f_{cp} = \frac{.000975}{.01670} = .0581$$

$$N_{pp} = 233 \qquad N_{cp} = 26 \qquad \text{from Fig. 1(a)}$$

$$\text{and} \quad \frac{.9419}{233} + \frac{.0581}{26} = \frac{1}{N_f} \qquad N_f = 159$$

This life compares with the measured value of 103 cycles, which is well within the commonly acceptable factor of 2. Note that this calcuation made no use of experimentally determined hysteresis loops or stress relaxation patterns. The calculations are still quite satisfactory, despite the neglect of transient creep, although the inclusion of transient creep did improve the predictions somewhat.

Fig. C shows a summary of calculations made by the above procedure for additional hold time tests taken from Ref. 4. The predictions agree well with the experiments. We also note that the degree of agreement between prediction and experiment does not decrease as the total test time increases.

Extension to Treatment of Low Strains and/or Long Hold Times

We shall now extend the same concepts already described in connection with the treatment of large strains to the study of low strains and long hold times. The elements of the procedure are:

a) The determination of the plastic strainrange from knowledge of the stress range and the log-linear life relations of elastic and plastic strainranges.

b) The determination of secondary creep strains by integrating the equations relating creep rate to a power-law of stress.

c) Determining transient (or primary) creep strains from actual observations of total creep during any interval and substracting the secondary creep strains. This step is optional, and is omitted if experimental facilities are unavailable or if a semi-experimental phase is inconvenient.

d) Constructing the strainrange components $\Delta\varepsilon_{pp}$, $\Delta\varepsilon_{pc}$, $\Delta\varepsilon_{cp}$ and $\Delta\varepsilon_{cc}$ from the determined creep and plasticity components in the tensile and compressive halves of the cycle.

e) Applying the Interaction Damage Rule to determine life.

Of special importance is the determination of the stress values that develop. To this extent the stresses will be known accurately either if directly measured by experimental observation of the hysteresis loop, or if accurate constitutive equations are available to track stress and strains during the cycle. However, in some cases neither approach will be practical; then the calculations will involve engineering approximations. We shall illustrate a case in which such approximations are required, their choice being made to introduce some conservatism in the resulting life estimates.

Combined Tensile and Compressive Hold Periods We first treat the case in which both tension and compression hold periods are introduced in problems involving low strainrange. It will be seen that this case lends itself more readily to the estimation of the hysteresis loop developed because of the symmetry of the cycle. Fig. 7 illustrates the procedure. We start with the recognition that because of the symmetry of the loading cycle, the hysteresis loop will be symmetrical in the tensile and compressive halves. Then the hysteresis loop will be ABCD for the strainrange $\Delta\varepsilon$. There, is, thus, only one unknown quantity in this analysis, for example σ_B. Once we know σ_B and the hold time, we can determine σ_C from the relaxation equation (7), and of course σ_D and σ_A follow from considerations of symmetry. Because of the non-linearity of the problem, however, it is convenient to start with the assumption of known stresses and to determine the combinations

of strainranges and hold times that will generate these stresses. For example, in Fig. 7, suppose we were concerned with the solution for a strainrange $\Delta\varepsilon$ = 0.5% and various hold times. A convenient approach is first to construct a complete hysteresis loop MABNCDM for an arbitrarily selected strainrange, say 1% under rapid cycling. This can readily be done from the cyclic stress-strain curve, (or the linear life relations for elastic and plastic strainrange under rapid cycling at the temperature of interest, e.g. the pp and el lines in Fig. 1(a).

Vertical lines AD and BC can then be constructed at equal distances from the vertical axis and at a strainrange of 0.5%, to determine the specific stress values σ_A, σ_B, σ_C, and σ_D. It can then be immediately determined what hold time t_H is required to relax σ_B to σ_C (or σ_D to σ_A). Since the partitioning of the hysteresis loop ABCD into creep and plasticity components can readily be accomplished (even when curvature is present along AB and CD), the strainrange components are easily established. Of course, because of symmetry, only $\Delta\varepsilon_{pp}$ and $\Delta\varepsilon_{cc}$ develop, and in fact for small $\Delta\varepsilon$ the inelastic strainrange developed is almost entirely $\Delta\varepsilon_{cc}$. In either case the life can readily be calculated from the Interaction Damage Rule. Thus the calculation provides one point relating the life to $\Delta\varepsilon$ and t_H. Additional points can be obtained from the same loop MN by selecting a new value of $\Delta\varepsilon$ and repeating the procedure to determine a new hold time and life. In a similar manner, by choosing a new value of $\Delta\varepsilon'$ (say ½%), and proceeding with a spectrum of choices of $\Delta\varepsilon$, a new series of corresponding values of hold-time and life values can be computed.

The calculations can then be depicted in their entirety as shown in Figs. 8 and 9. We shall discuss these figures later, after presenting results for calculations involving hold times only in tension or only in compression.

Tensile Hold Periods Treatment of only tensile hold problems is not as straightforward as symmetrical tensile and compressive holds because of ambiguities that develop in the rheological behavior at low stress ranges. Consider, for example, the two extremes of behavior possible when a specimen is cycled at low strainrange and tensile hold periods are introduced. In Fig. 10(a) the behavior is depicted as involving little or no

plasticity during the reversal because of the small strainrange involved. In the first loading the stress-strain path is along OA. Although, according to the procedure adopted herein, all stress applications imply plastic strain (e.g. see Fig. 4(c)), the actual amount of plasticity is negligibly small if the total strainrange is small enough; therefore we show line OA as a straight line. A hold period at the maximum strain can, however, result in stress relaxation to point B, if the hold period is long enough. Thus, upon reverse loading the path is BC, which we again assume to be at strainrange low enough to preclude significant plastic deformation, causing BC to be a straight line. Since there is no hold period at C, and reloading is assumed to occur as rapid as possible, the subsequent loading is along the identical line CB. During the hold period relaxation again occurs along BD, an amount smaller than AB because the stresses involved are lower and times are assumed to be the same. The process is then repeated in subsequent cycles, each time the maximum tensile stress becoming lower and the maximum compressive stress becoming higher. Eventually a quasi-stabilized condition may be achieved along FG, wherein the stress at F is low enough to preclude appreciable further stress relaxation. But in principle, at least, the maximum stress can continue to relax during the hold period, eventually approaching zero. Thus the final stabilized condition involves no cyclic inelasticity involving creep, and extremely small plasticity dependent only upon the strainrange. With the small plasticity developed, and the negative mean stress along F' G' the fatigue life can become very long. In fact, the longer the hold time the lower will be the number of cycles required to stabilize to the low peak tensile stress, assuming this type of rheological behavior. Thus, assuming this type of behavior, the longer the hold time the higher the possible cyclic life.

The other extreme of behavior is shown in Fig. 10(b). Here it is assumed that the stabilized loop becomes PQR and that the creep relaxation during PQ somehow, either because of the deformation or the high temperature exposure, softens the material in reversed loading, so that QR develops the plasticity required to balance the creep occurring during PQ. The specimen thus develops a $\Delta\varepsilon_{cp}$ strainrange. Obviously the higher the stress at P, the higher will be the $\Delta\varepsilon_{cp}$ strainrange, and the lower the cyclic life, for a

given hold time. In general, it can be expected that the peak compressive stress at R will be higher in magnitude than the peak tensile stress at P. Thus the lowest cyclic life will result when σ_p is as close as possible to σ_R, say equal. The life in this case can become substantially lower than that for the cycling of Fig. 10(a) and along F' G'.

From the above discussion it is apparent that the factor that most significantly governs fatigue life is the rheological response of the material to the imposed loading, not so much the method of calculating the life once the rheological response is known. This area of establishing accurate constitutive response to know imposed loading is a very important subject, and requires much further study. However, in order to treat the problem in a conservative manner it will be assumed that case 10(b) actually develops, and that σ_p is half the stress range that is calculated for the strainrange $\Delta\varepsilon$, as determined from the double-amplitude concept of constructing hysteresis loops from the basic life relation lines. For small strainranges the maximum stress will be approximately the product of elastic modulus and half of the strainrange; but the approach using the double-amplitude concept will be valid even for larger strainranges wherein curvature develops along the loading path.

Figures 11 and 12 show the results of conservative life calculations made for a spectrum of strainranges and hold times assuming the rheological behavior to be that of Fig. 10(b). For each selected strainrange the line PP was first constructed according to the double-amplitude loading path concept, and the stress range determined. The stress at P was assumed to be half the stress range involved, and starting with this time the relaxation PQ was determined using Eq. (6) for the known hold time. The exact shape unloading path QR did not enter into the calculations except that the initial portion of the unloading QS is parallel to an elastic line. Thus the strain developed is a $\Delta\varepsilon_{cp}$ equal to the relaxed strain during the PQ, and a $\Delta\varepsilon_{pp}$ strain associated with any curvature developed along RP (negligible for low strains, but included in the calculations shown for the large strainranges).

Compressive Hold Periods Treatment of hold periods imposed only during the compressive peak strain is identical to that for tensile hold periods. The rheological calculations are the same, and the dilemma regarding actual response to imposed loading is also the same; the only difference is that $\Delta\varepsilon_{pc}$ develops for compressive hold, whereas $\Delta\varepsilon_{cp}$ develops for tensile hold. The life relationships are, therefore, different. Results of the calculations are shown in Figs. 13 and 14.

Continuous Cycling As a final example of extension of SRP analysis to low strainranges we consider continuous cycling over a range of frequencies. If the cycling is carried out by controlling the strain rate, for example, at a uniform rate of either total strain or inelastic strain, as has been common in many recent experimental programs, a means is required to establish the stresses that develop. Either accurate constitutive equations or the quasi-experimental approach of determining the stabilized hysteresis loop provides the necessary stress information to proceed by the principles already described. If the problem is one in which the stress pattern is specified, then no further rheological information is needed to perform the analysis. In the following illustration we shall assume the stress is symmetrically ramped linearly to selected tension and compressive peak values. The strain levels are not specified; rather they are derived from the stresses and ramping rates as the consequential combined creep and plasticity values. To analyze the data, and to cast them in a form commonly used in creep-fatigue analysis, however, they are cross-plotted to obtain life along lines of constant strainrange.

A sample computation is detailed in Fig. 15. The frequency is 10^{-5}Hz, and a stress amplitude of 17ksi at a temperature of 1300F is assumed. Since the stress is ramped linearly its value is known at each instant, and the creep is calculated in step 1 from the known creep rate relation in terms of the power-law of stress. Steps 2 and 3 utilize the known stress range to determine plastic strain range, using the life relations. From symmetry $\Delta\varepsilon_{pp}$ and $\Delta\varepsilon_{cc}$ are determined in Step 4, and f_{pp} and f_{cc} in steps 5 and 6. The Interaction Damage Rule is then applied in step 7 to obtain life. Thus,

as shown in Fig. 15(b) the point P or the line of 10^{-5}Hz can be plotted with $\Delta\varepsilon_t$ = .00398 and a cyclic life of 4,398 cycles. Other points along the 10^{-5}Hz curve can be obtained by selecting additional values of peak stress and repeating the calculations. In this manner the complete curve for 10^{-5}Hz as well as other frequencies were established. The results are shown in Fig. 16. Cross-plots of the information in Fig. 16 are shown in Fig. 17 with strainrange as a parameter are shown in Fig. 17. In Figure 17 the numbers next to the tick marks represent the selected stress amplitude that generated that point.

Results of calculations for 1200F are shown in Figs. 18 and 19, which are analogous to Figs. 16 and 17. These calculations provided a means to make a comparison between calculations made in this manner with experiments available from the literature. Although the literature results (Ref. 4, p 38) were obtained by ramping total strain at a constant rate, while the calculations were made for constant stress rate ramping, the agreement is very good when the comparison is shown in Fig. 20. It is seen that the degree of agreement is about as good at the low values of strainrange as at the high values, and at the high values of total test time as at the low values.

Discussion The foregoing calculations show that Strainrange Partitioning readily lends itself to the treatment of low strainranges and long hold times. The principles involved in such calculations are similar to those used in the treatment of large strains. Where direct comparison between calculations and experiment has been possible, the agreement has been very good. An important point in this connection is that the data entering into these calculations are totally independent of the experiments predicted. Thus, for example, the tests conducted to determine creep strain rate as a function of stress, and the generic SRP life relations, are totally independent of the hold time and continuous cycling tests predicted. In fact the tests were conducted by different investigators in different laboratories on separate lots of material. The fact that agreement is obtained at the strainranges where data are available, despite the diversity of testing conditions involved in basic data generation and experiments

conducted in comparison to predictions lends some credence to the concepts of Strainrange Partitioning. However there has been no opportunity to check predictions against test results involving very low strainranges or very long hold times. Since these calculations involve the extrapolation of the SRP life relations to low strain values as well, it is apparent that experimental verification is required for the approach discussed. Not only the basic life relations and the procedure, but the rheological behavior so important in governing the parameters that enter into the calculations, require future study.

Some interesting results and problems raised by the calculations will now be discussed. Figures 8, 11, 13, 17 and 19 show the effects on cyclic life of varying hold times for selected values of total strainrange. For the high strainranges the effect of long hold is relatively small because longer hold only causes conversion of a small percentage of the total imposed strainrange into the more detrimental cp, pc, or cc strainrange components. But at the low strainranges the effect can become appreciable. For example, for 316 SS steel at 1300F subjected to symmetrical hold in both tension and compression, Fig. 8 shows that at a .05% strainrange life can be reduced by more than a hundred-fold for a hundred-fold increase in hold time from 10 hrs to 1000 hrs whereas at 0.1% strainrange this change in hold time only reduces life by less than a factor of 10. But note, also, the high life values involved. Even with hold times of 1000 hrs, 10,000 cycles can be sustained at a strainrange of 0.1%. The total time is enormous. Plotted in Figs. 8 to 19 is a dotted curve representing 30 years of life. Note that the large effects involved time ranges wherein the method cannot be expected to be accurate because of the simplified assumptions involved and because of inevitable metallurgical changes.

In general, all life values tend to saturate at higher hold times as the total imposed strainrange tends to be converted to the most detrimental type involved in the application (i.e. cc in symmetrical hold, Fig. 8; cp in tensile hold, Fig. 11; pc in compressive hold, Fig. 17; and cc in stress ramping, Fig. 19).

Of special interest, too, is the relative damage of the various types of hold period patterns possible. Note, for example, by comparing Figs. 11 and 13, that while tensile hold is more damaging than compression hold in the high strainranges, the compressive hold is more damaging in the low strain-ranges. The reason for this lies in the slopes of the life relationships for this material. Since the slope for the pc life is steeper than that for the cp life, extension to low strains causes the two to intersect and to diverge in opposite directions at low strains compared to the high strains. The transition occurs at a strain range of about .035%. This type of behavior has already been noted in the past for 2¼ Cr - 1 Mo steel for which pc was noted to be more damaging to cp behavior at even higher strain-ranges in the order of 1%. However, the slopes of the two life relations were also unequal, and at considerably higher strainranges it appeared that cp damage could also exceed the pc value. Thus it may well be that each material has its own cross-over value, and it is important to study low strains in order to obtain further insight. However, it should be noted that from a practical viewpoint the crossover for 316 stainless steel occurs at times which are outside the usual range of practical interest. The matter has only academic value.

A comparison of Figs. 8 and 11 is also interesting in this respect. At the high strain ranges of the order of ½% and higher, the tensile hold appears to be more damaging than the combined tensile and compressive hold. At a strainrange of 0.1%, tensile holds also seem more damaging than symmetrical holds at hold periods of 3 hrs or less, but less damaging for hold periods above 3 hrs. At a strain range of 0.05% symmetrical holds appear to be more damaging than tensile holds over the entire range depicted. Again this is a reflection of the linear extrapolation of the life relationships into the low strainranges, and requires checking. In addition, it should be recalled that as discussed in connection with Fig. 10, tensile hold alone can result in favorable stress relaxation which reduces undesirable tensile stress. The calculations shown in Fig. 11 were made for the conservative assumption indicated in Fig. 10(b) that the maximum tensile stress equals the compressive stress. Thus it can be seen that even with conservatism the effect of tensile hold is not as detrimental at the low

strains and long hold times relative to symmetrical holds in tension and compression as would be expected from test results at high strainranges. Note also that as strain is decreased lives increase substantially, but that most of the plot relates to times above the 30 year range of interest.

Figures 9, 12, 14, 16, and 18 show the same calculations with hold-time as the parameter. These plots are analogous to conventional plots of total strainrange vs cyclic life which reflect two regions -- one in which the inelastic strainrange predominates, the other in which the elastic strainrange predominates. At the high strain ranges, where the inelastic strainrange predominates, all the curves are steep, and relatively insensitive to hold time. Most of the strain is induced as the pp type, and hold time introduces only moderate amounts of cp, pc, or cc strain (depending on the type of hold pattern). Thus the life is little affected. The inelastic lines do increase somewhat in slope as hold time is increased in contrast, for example, to remaining parallel (as required by the Frequency-Modified Life Equation). In the low strainrange level we again see near-linearity, but the lines fan out with considerable increase in slope as hold time is increased. Thus the "elastic-line" analogue, by Strainrange Partitioning, is one of considerable varying slope and depends strongly on the nature of the hold period. But the very large differences in hold-time effect occur at nominal times beyond 30 years.

The above behavior cannot, of course, presently be checked by experiment. However, we can compare the predictability in the time and strainranges that have been studied as an indication of what to expect as strainrange is decreased or total test time increased. Some results are shown in Figs. 5, 6, and 20. Each figure shows that a reasonable agreement occurs between the predictions and experiments for the time and strainranges that have been studied herein. If the ratio of experimental life to predicted life is plotted against either strainrange or hold time, these limited data do not indicate any reduction in corservatism either as strainrange is decreased or total test time increased. Further experiments to extend the ranges of strain and hold time are, of course, needed for conclusive results. Figures 11 to 19 should not be interpreted as final predictions by SRP, since there are many variables that have not yet been incorporated

into the calculations, such as ductility variations later to be discussed. The main point of the figures is to indicate that a simple procedure is available to calculate idealized lives according to the method, but that further research is needed to incorporate additional realistic features.

ADDITIONAL CONSIDERATIONS

The foregoing discussion was intended to indicate procedure for calculations, rather than to provide accurate final design information. Figures 8, 9, and their subsequent counterparts are, for example, very sensitive to extrapolation of life relations which are presently based on relatively little information in the high strain and short life range. If similar figures were to be constructed for design use it would, of course, be necessary to extend the data base upon which the calculations are made. We consider in the following brief discussion several other factors in addition to the more accurate determination of the life relations and constitutive equations already emphasized.

Environmental Effects

Environment is, of course, a major factor in governing fatigue life, especially when dealing with long-time applications. It is well known that the presence of oxygen can substantially reduce fatigue life, and that fatigue in vacuum or inert environment is usually considerably better than in air. In fact, it has been suggested by some investigators that high temperature fatigue degradation is entirely an oxidation effect. This proposal was based on the fact that the high temperature fatigue properties of numerous materials in vacuum were about the same as their room temperature fatigue properties in air, thereby pointing to oxidation as the degrading influence. However, all the fatigue tests on which this conclusion was based were of the continuous cycling type, inducing only pp and cc strains. One of the major contributions of Strainrange Partitioning was to point to the need for loading cycles producing pc or cp strains in order to bring out the fact that even in vacuum large degrading influences of the creep fatigue interaction could result. A number of alloys have been studied in high vacuum, among them the refractory alloys T-111 and Astar 811C (Ref. 6), A286 and 304 stainless steel (Ref. 7), and Rene' 80

(Ref. 8). All have shown that a creep fatigue interaction occurs even in vacuum. In general, an air environment reduces the fatigue properties below the corresponding properties in vacuum for the same type of strainrange. The refractory alloys cannot, of course, operate in air at high temperature because of their severe oxidizing tendencies; there is no point, thus, in comparing the fatigue properties under the two environments. The iron base alloys A286 and 304 stainless steel improved in vacuum relative to air. The nickel base alloy Rene' 80 showed only minor degradation in air, however, because of its general oxidation resistance, large grain size, and low ductility in both environments. Only the pp life relations fall appreciably in the air environment, and even a coating to protect from oxidation did not prevent this degradation. The results require further analysis before they can be completely explained. From all the tests referred to above, the major conclusion emerged that while the properties are different in the air and vacuum environments, each material yielded to the determination of pp, cp, pc, and cc life relationships in each environment. Analysis using these life relations permitted the correlation of all the data obtained within that environment. Thus SRP was useful in analyzing data in a vacuum environment as well as air.

Another point of significance in this respect was discussed in Chapter 4 of Reference 1. There it was pointed out that such fatigue degradation as occurs from oxidation develops in relatively short time and requires relatively little oxygen. Corroboration was drawn from published research on aluminum showing that a sharp discontinuity in the fatigue response occurred within a narrow range of pressure (about 10^{-2} to 10^{-3} Torr). Above this pressure the fatigue response was very little different from that in atmospheric air (760 Torr), and below this pressure it was very little different from that in the high vacuum of 10^{-8} Torr. Thus it appeared that if enough oxygen atoms were available to oxidize the freshly exposed surface caused by the plastic deformation leading to fatigue, increasing the amount by a thousand-fold did not accelerate the process appreciably. From this it might be possible to deduce that extended periods in air do not necessarily degrade fatigue much more than modest exposures, as long as these exposures provide the

critical amount of oxygen required for the basically rapid oxidation. If it is assumed that the normal determination in air of the basic SRP life relationships involves conditions adequate to provide the minimum oxygen requirements, then it can be concluded that little correction will be required to apply these relationships in analyzing long time tests.

Evidence that the above reasoning may be valid is shown in Fig. 21. These were data interpreted by Halford (Ref. 9) in analyzing the Interspersion tests of Curran and Wundt (Ref. 10) sponsored by the Metals Properties Council. The tests were basically of the cp type of loading, and in analyzing the results Halford used the cp and pp life lines for the 2¼ Cr-1 Mo steel determined at NASA (Ref. 3) in tests lasting 100 hours or less. Yet the predictions of the MPC data testing up to 5000 hours yielded approximately the same degree of correlation as the short tests. A small tendency for the experimental results to fall somewhat shorter of the predictions in the longer time range than in the short time range may be discerned in Fig. 21, but this point needs further study. Note, however, that at an extrapolation in time by a factor of 30, the agreement is still very good.

It might be deduced from the above discussion that in conducting the tests to determine the life relations for use in the SRP analysis discussed in the earlier section of this report, the times involved should be of the order of 1/10 to 1/50 of the desired extrapolation times in order to insure reasonably valid extrapolations. This is quite practical. If the tests take as much as one to three years, extensions to 30 years may be achievable. It thus appears reasonable to suggest that the basic SRP relations be generated from tests requiring approximately a 1-3 year duration. Load-holding tests to generate the cp, pc, and cc life relations can then use quite long hold-times in each cycle to consume the time required to cause the tests to be protracted to this duration. If the creep can be measured directly, then of course this should be done. If not, use of the power-law relation between stress and creep rate discussed earlier in this report can be applied by extrapolation to low stresses.

Vacuum tests can also serve a useful purpose. First, by changing the pressure over a wide range, information can be obtained as to how much oxygen exposure is required to produce varying degrees of oxygen degradation on fatigue. Also such tests can help determine how much benefit might be achieved from the development of coatings or other surface protection systems which exclude oxygen, although the question of surface coatings is complicated by metallurgical interaction between coating and substrate, and by the notching effect if the coating cracks.

Metallurgical Effects

Another factor that requires consideration is the metallurgical effect beyond the chemical interaction represented by surface oxidation. Phase precipitation, for example, may have a number of effects. Ductility may change, thus influencing fatigue. Or precipitates may change the creep resistance, thereby altering the creep rates in later cycles. In particular, if the precipitates occur in the grain boundaries, they can seriously alter the cp, pc, and cc life relations. Thus care should be exercised to insure that any expected instabilities are accounted for in extending the life relationships to unexperienced time levels. Some reference to this subject has already been made in Chapter 4 of Reference 1. Two important effects were discussed. One of these is that temperatures which can either degrade or enhance ductility could seriously alter fatigue life. In Fig. 4.43 of Ref. 1 it was observed, for example, that in the temperature range of 1100 to 1500F, IN-706 is associated with low ductility because of an oxidation-enhanced precipitate. The universalized SRP life relations, which use ductility as a normalizing parameter, suggest a quantitative reduction in fatigue in air within this temperature range. In vacuum, however, the oxygen-enhanced precipitate does not occur; the ductility is not reduced; and the fatigue properties do not suffer. Elevating the temperature above 1500F, however, avoids the precipitation enhancement range, and the fatigue does not suffer at all. Thus the beneficial effect of vacuum is in suppressing the precipitation tendency, not protecting against surface oxidation. It is important to be alert to this factor in studying low strain and long time extrapolation because the effect may be both strain- and exposure time-dependent.

The second point discussed in Chapter 4 of Ref. 1 is that it may be possible to improve the fatigue characteristics involving the creep mode by causing a suitable precipitate to develop in the grain boundaries. It was point out, for example, that the T-111, while similar in composition to the ASTAR 811-C, does not contain a precipitate in the grain boundary whereas the latter does. The fatigue properties in the modes involving creep are much better for the material containing the precipitate which retards grain boundary sliding. Thus we have a clue as to how to improve fatigue resistance through the incorporation of a grain boundary precipitate.

Similar consideration should be given to grain size effects in this context. The larger the grain size the less will be the tendency for grain boundary sliding, and the more a given imposed strain will be absorbed in the less detrimental pp deformation. Thus it appears that some control is available to influence fatigue properties by heat treatment to develop optimal grain size. It would be desirable to study various processing variables such as working and heat treatment, either individually or in conjunction with each other, to determine optimum combinations for resisting high temperature creep fatigue interaction. Strainrange Partitioning offers some guidance as to the desired effect by regarding the interaction to a first approximation as one involving the interchange between slip plane sliding and grain boundary sliding. It would then appear that larger grains to minimize grain boundary areas, the development of a precipitate to impede grain boundary sliding, and thermomechanical processing to enhance creep and tensile ductility are desirable directions of approach.

One of the advantages of Strainrange Partitioning as a means of treating the creep-fatigue interaction is that it provides a framework for including the possible effects of ductility variations during the service life of the component being analyzed. Since the universalized life relations are normalized with respect to ductility, changing ductility can be included by considering small time increments during which ductility can be regarded constant. The approach was first used in Ref. 11 to treat frequency effects in A-286 which was known to have a time-dependent creep ductility. The results are summarized in Fig. 22 (taken from Ref. 11). Note

that the Ncc life curve changes with frequency because the life depends on frequency, which in turn governs creep ductility. The effect was to produce a lower cyclic life at the low frequencies than would have been predicted if creep ductility did not change with life, because the lower the frequency the longer is the chronological life (i.e., hours, not cycles), and this reduces the effective creep ductility.

The method was also used in Chapter 4 of Ref. 1 to provide a guideline as to the possible general effects of ductility reductions during the lifetime of a component. In this case the calculations were based on linear reductions in ductility with time. The results are summarized in Fig. 23, taken from Fig. 4.88 of Ref. 1. Two situations are presented: in Fig. 23 (a) is shown the reduction in life as a function of ductility reduction during the lifetime of the part. For example, it is seen that if the ductility at the end of the intended design life is 50% of the initial ductility, the design life will be reduced by 25 to 30%, depending on whether the exponent in the life relation is 0.6 (i.e. typical of the pp life), or 0.8 (typical of the cp life). Figure 23(b)* shows another way of representing the effect. It shows the required reduction in strainrange to maintain life at design value. Thus, for example, if the ductility at the end of the design life is half of the initial ductility, the initial design life can be maintained if the strain is reduced to about 2/3 the design value based on no ductility degradation due to environmental effects.

In the present study we carried out the ductility calculations to include what would happen if the decay was exponential. A brief description of the procedure is outlined in Appendix A. The calculations are summarized in Figs. 24 and 25. Figure 24 shows the hypothesized ductility decay curves, identified by "half-life" i.e. the time required for ductility to decay to half its initial value. This type of ductility degradation is not typical; it is more common for ductility to remain fairly constant in the

*This figure differs from that of Ref. 1, correcting for a typographical error, and minor numerical discrepancies.

early period of exposure, and to drop off only after some undesirable precipitates have had a chance to develop. Figure 25 shows the predicted life based on exponential decay vs the design life based on constant ductility, using the two characteristic exponents associated with the universalized Strainrange Partitioning life relations (i.e., 0.6 to typify pp strain, and 0.8 to typify the others). It is seen that the results are relatively insensitive to the value of the exponent, suggesting that the curves would apply to all combinations of strainrange components found in specific problems (provided, of course, the assumption is made that if ductility losses occur, these losses are applicable to both plastic deformation as well as creep). Note, however, that drastic reductions in life are possible if losses of ductility are high enough. For example, a design life of 30 years can become a service life of 3-4 years if the ductility half-life is one year. This, of course, is not expected for materials actually used in reactors, but it indicates how important it is to assure that drastic losses of ductility be avoided.

SUMMARY AND CONCLUDING REMARKS

In this report we have attempted to outline a simple procedure for treating creep-fatigue for low strainranges and long hold times. We have suggested that a semi-experimental approach, wherein several cycles of the imposed loading is actually applied to a specimen in order to determine the stable hysteresis loop, can be very useful in the analysis. Since such tests require only a small fraction of the total failure time, they are not inherently prohibitive if experimental equipment is available. It is, in fact, a simple method of by-passing the need for accurate constitutive equations since the material itself acts to translate the imposed loading into the responsive hysteresis loops. When Strainrange Partitioning has been applied in such cases very good results have been obtained.

Since in many cases a concomitant experimental program is impractical, a simple procedure is outlined for handling the problem entirely by

analysis. Some approximations are involved, of course, which require further checking. Calculations shown include continuous cycling, tensile holds, compressive holds, and symmetrical tensile/compressive holds. Constant strain-range curves of cycles to failure vs hold time display the familiar tendency to saturate at both very short and long hold times, with an S-shaped pattern over a large range of hold times. Similarly, constant frequency curves of strainrange vs cycles to failure are of a familiar shape, being asymptotic to two straight lines on logarithmic coordinates like the sum of an elastic and an inelastic component. Each family of lines shows the characteristic increases in slope as hold time is increased, a feature observed in the shorter time range by several investigators. While these figures are presented merely as sample results of a calculation procedure, rather than accurate predictions, they may serve as guides to the selection of critical experiments to compare predictions of SRP with alternative methods.

Oxidation effects are not directly included in the computations, except that the constants involved in the calculations are obtained in the environment of interest. Although long term exposure can be expected to accentuate the oxidation, or to promote metallurgical precipitation that can seriously affect fatigue life by influencing mechanical properties such as strength, toughness, and ductility, these factors were not included in the calculations. The SRP framework does, however, allow for inclusion of such effects if they are known or expected to occur. Chapter 4 of Ref. 1 first suggested how such calculations might be carried out. It should also be pointed out, however, that in several analyses where it has been possible to make comparisons, the degree of predictability by the SRP approach of long-time results is little different from that of short-time results. Figure 21 suggests, for example, that extrapolations by a time factor of 10 to 50 may be reasonable. This conclusion must, of course, be extensively checked before confidence can be established. However, it would seem reasonable to assume that if extrapolations are to be made to the 30 year range, then the life and creep rate relations should be determined from tests lasting 1 to 3 years, an attainable requirement.

We have also extended in this report the application of Strainrange Partitioning to the treatment of problems involving progressive loss of ductility due to environmental exposure. In addition to the previous analysis of Chapt. 4 of Ref. 1 wherein linear reduction in ductility with time was treated, we have extended in this report the treatment of ductility variations to include the case of exponential loss with time. This is an extreme case, not exptected in service, but it illustrates the importance of choosing stable materials that do not suffer drastic losses in ductility during their early exposure.

ACKNOWLEDGEMENT

In addition to subcontract support from Oak Ridge National Laboratory, this research was supported, in part, by a grant from the NASA Lewis Research Center (M. H. Hirschberg, Grant Monitor).

REFERENCES

1. Carden, A.E., Coffin, L.F., Manson, S.S., Severud, L.K., Greenstreet, W.C., "Time-Dependent Fatigue of Structural Alloys", ORNL-5073, 1977.

2. Halford, G.R., Hirschberg, M.H., Manson, S.S., "Temperature Effects on the Strainrange Partitioning Approach for Creep-Fatigue Analysis", Fatigue At Elevated Temperatures, STP-529, ASTM, 1973.

3. Manson, S.S., Halford, G.R., and Hirschberg, M.H., "Creep-Fatigue Analysis by Strainrange Partitioning", Proceedings of First Symposium on Design for Elevated Temperature Environment, San Francisco, California, May 10-12, 1971, pp. 12-24; disc. pp. 25-28 (1971).

4. Conway, J.B., Stentz, R.H., and Berling, J.T., "Fatigue, Tensile, and Relaxation Behavior of Strainless Steels", United States Atomic Energy Commission, 1975.

5. Manson, S.S., Halford, G.R., Nachtigal, A.J., "Separation of the Strain Component for Use in Strain Range Partitioning", published in Advances in Design for Elevated Temperature Environment, ASME, 1975.

6. Sheffler, K.D., Doble, G.S., "Influence of Creep Damage on the Low-Cycle Thermal-Mechanical Fatigue Behavior of Two Tantalum Base Alloys", NASA-CR-121001, May 1972.

7. Sheffler, K.D., "Vacuum Thermal-Mechanical Fatigue Testing of Two Iron Base High Temperature Alloys", NAS CR-134524, TRW ER 7697, NASA Topical Report #3, (January 1974).

8. Kortovich, C.S., "Ultrahigh Vacuum, High Temperature, Low Cycle Fatigue of Coated and Uncoated Rene' 80", NASA Report NAS CR-135003, TRW ER-7861, (April 1976).

9. Saltsman, J.F., Halford, G.R., "Application of Strainrange Partitioning to the Prediction of MPC Creep-Fatigue Data for 2¼ Cr-1Mo Steel", NASA Report TM X-73474, December 1976.

10. Curran, R.M., Wundt, B.M., "Continuation of a Study of Low-Cycle Fatigue and Creep Interaction in Steels at Elevated Temperatures", MPC-ASME Symposium on Creep-Fatigue Interaction, December 1976.

11. Manson, S.S., "The Challenge to Unify Treatment of High-Temperature Fatigue a Partisan Proposal Based on Strainrange Partitioning ASTM-ASME, STP 520 1973.

BLANK PAGE

Appendix A

The ductility equation which is a function of time(t) is

$$D_t = D_o e^{-at}$$

D_t = Ductility - t years

D_o = Original ductility

a = Constant (function of half-life)

t = time (years)

The strain equation is

$$\frac{\Delta\varepsilon}{D_t} = A N^{-\alpha}$$

Solve for N (number of cycles)

$$N = \left[\frac{A D_o e^{-at}}{\Delta\varepsilon}\right]^{\frac{1}{\alpha}}$$

Damage equation is

$$\int_0^y \frac{A D_o e^{-at}}{\Delta\varepsilon}^{-\frac{1}{\alpha}} n dt = 1$$

n = Number of cycles, per year

α,A = Constants of material

$\Delta\varepsilon$ = Strain Range

y = Years to failure if ductility decreases

Integrate and substitute limits.

$$\frac{AD_o}{\Delta\varepsilon}^{-\frac{1}{\alpha}} \frac{n^{\alpha}}{a} e^{\frac{a}{\alpha}y} - 1 = 1$$

Eq. (1)

Let $$N_o = \left[\frac{A D_o}{\Delta\varepsilon}\right]^{(1/\alpha)}$$

Eq. (2)

be the number of cycles if no change in ductility occurs. Substitute equation (2) into equation (1) and solve for y.

$$y = \frac{\alpha}{a} \text{ Ln } (\frac{a}{\alpha} \frac{N_o}{n} + 1)$$

Also

$$N_o = ny_o$$

n = number of cycles per year

y_o = number of years to failure if there is no decrease in ductility

Therefore

$$y = \frac{\alpha}{a} \text{ Ln } (\frac{a}{\alpha} y_o + 1)$$

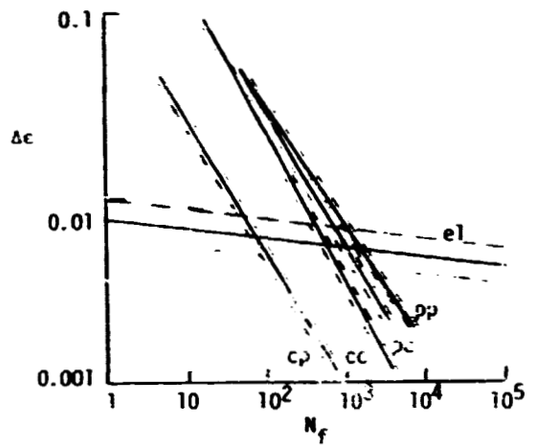

a) Partitioned Strainrange Life Relations

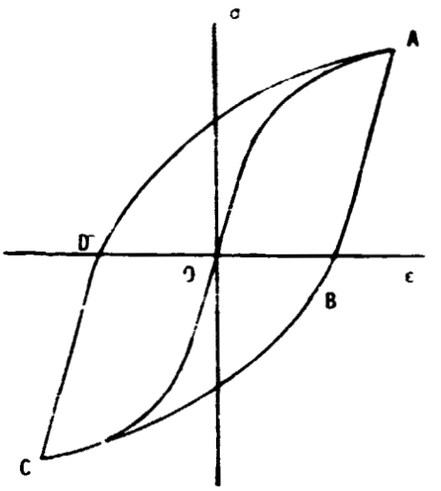

b) Cyclic stress-strain curve and Hysteresis Loop for Rapid Cycling obtained by Principle of Double Amplitude Construction

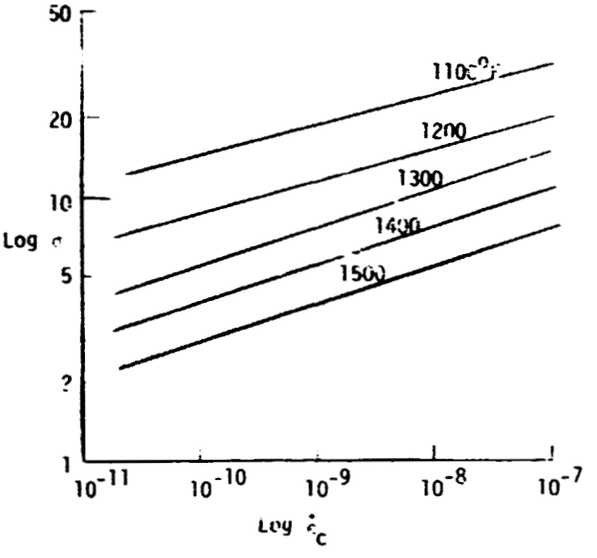

c) Relation between Steady State Creep Rate and Stress

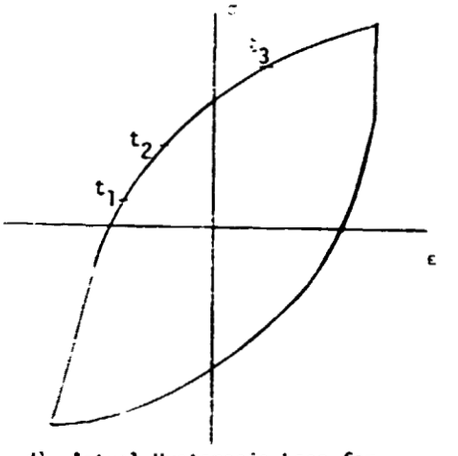

d) Actual Hysteresis Loop for Cycle of Interest

Fig. 1. Desired Input Information for Treating Creep-Fatigue by Strainrange Partitioning

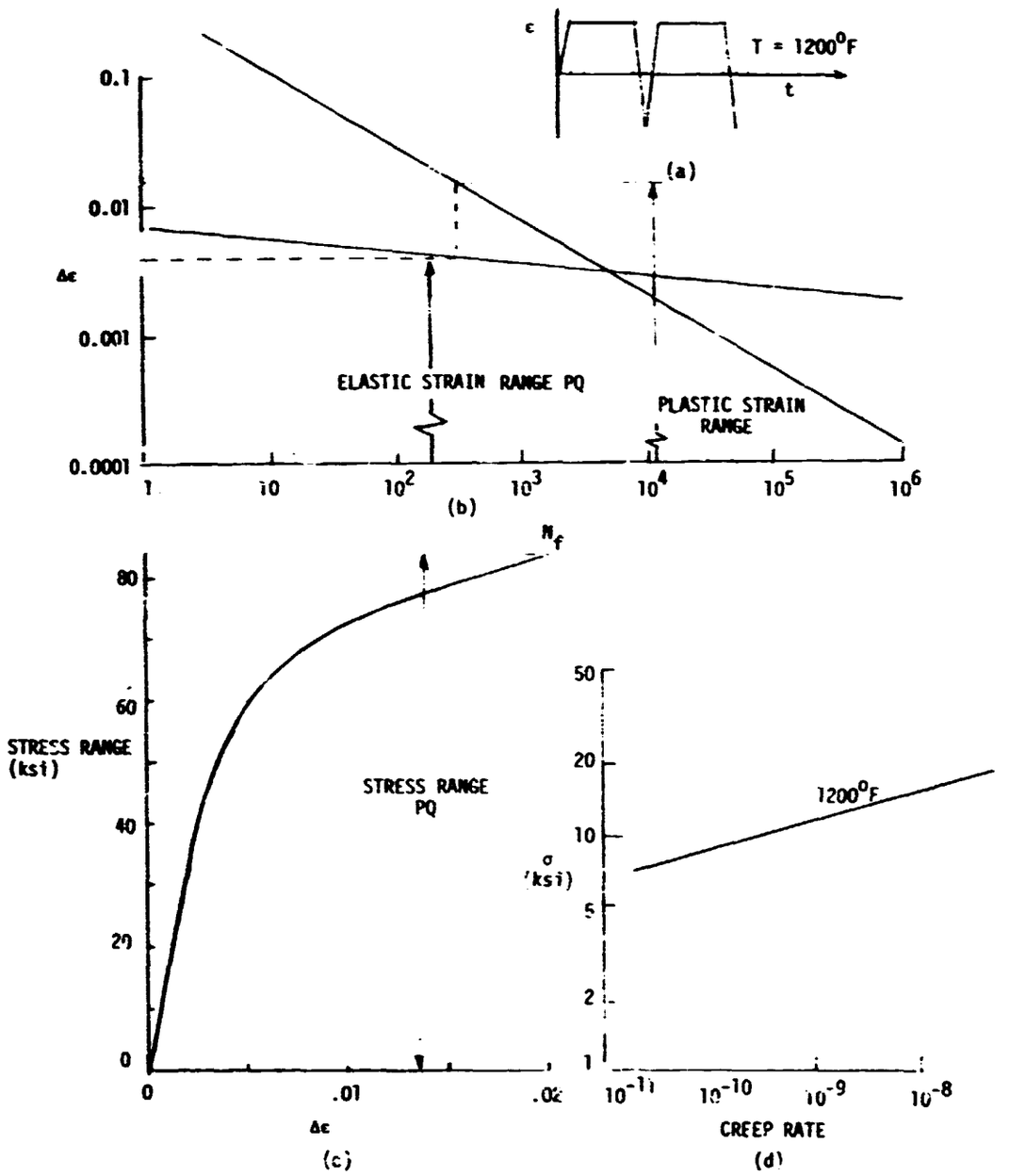

Fig. 2. Input information for analysis of hold-time test.

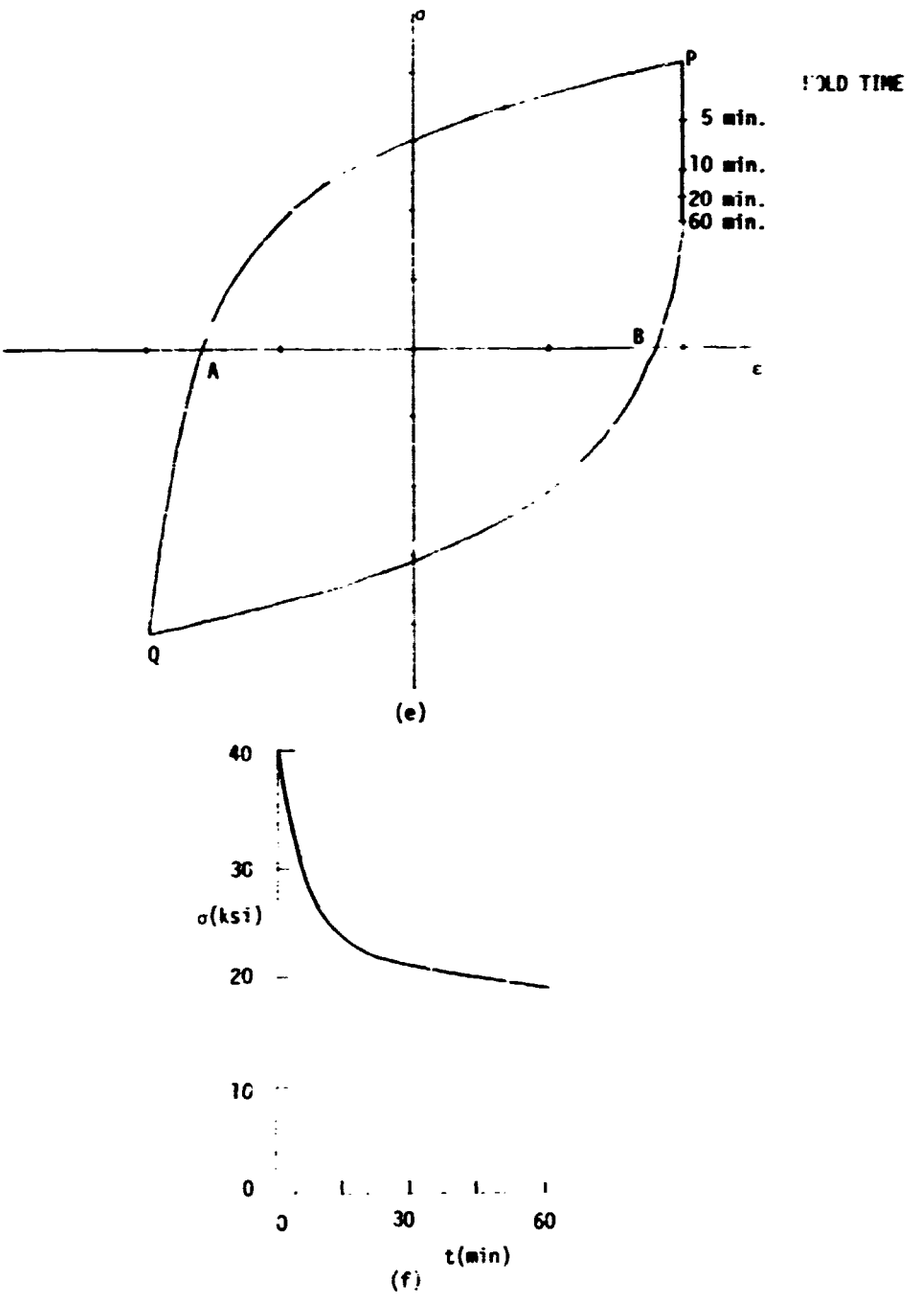
σ
P
HOLD TIME
5 min.
10 min.
20 min.
60 min.
B
A
ε
Q
(e)
40
30
σ(ksi)
20
10
0
0
30
60
t(min)
(f)

Fig. 2 (cont.)

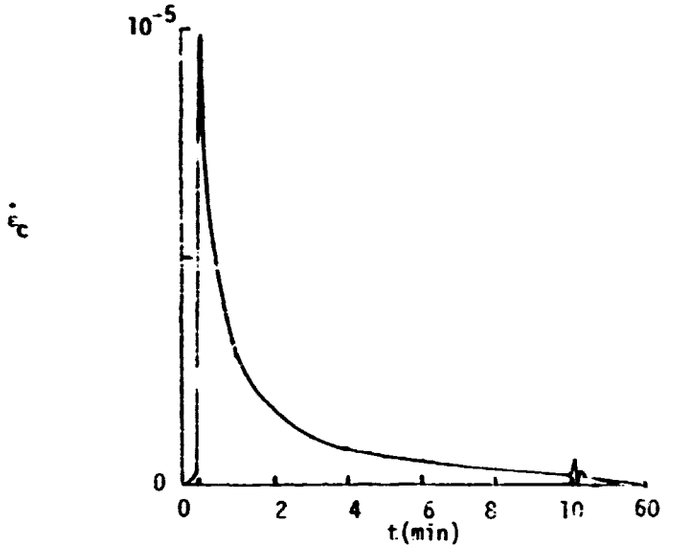

a) Tensile secondary creep = area under creep rate curve
$= (9.75 \times 10^{-4})$

Elastic stress range = 83.74 ksi

b) Elastic strainrange = $\frac{83.740}{21.1 \times 10^6} = 3.96 \times 10^{-3}$

From Fig. 2(b) Plastic strainrange = 1.60×10^{-2}

c) From Fig. 2(e), total inelastic strainrange = AB = 1.67×10^{-2}

d) Transient creep strainrange = total inelastic strainrange - plastic strainrange
$= 1.67 \times 10^{-2} - 1.60 \times 10^{-2} = 7 \times 10^{-4}$

e) Total tensile "creep" for SRP purposes

= tensile secondary creep + 0.1 x transient creep
$= 9.75 \times 10^{-4} + 0.1(7 \times 10^{-4}) = 1.045 \times 10^{-3}$

f) Total compressive creep for SRP purposes = 0

g) $\Delta\varepsilon_{cc} = 0$

h) $\Delta\varepsilon_{cp} = 1.045 \times 10^{-3}$

i) $\Delta\varepsilon_{pp}$ = Total inelastic strainrange minus $\Delta\varepsilon_{cp} = 1.5655 \times 10^{-2}$

j) Thus $F_{pp} = .9374$ $F_{cp} = .0626$

k) Using Interaction Damage Rule $\frac{.0626}{26} + \frac{.9374}{233} = \frac{1}{N_f}$ $N_f = 155$

Fig. 3. Numerical Analysis of Strain-hold Problem.

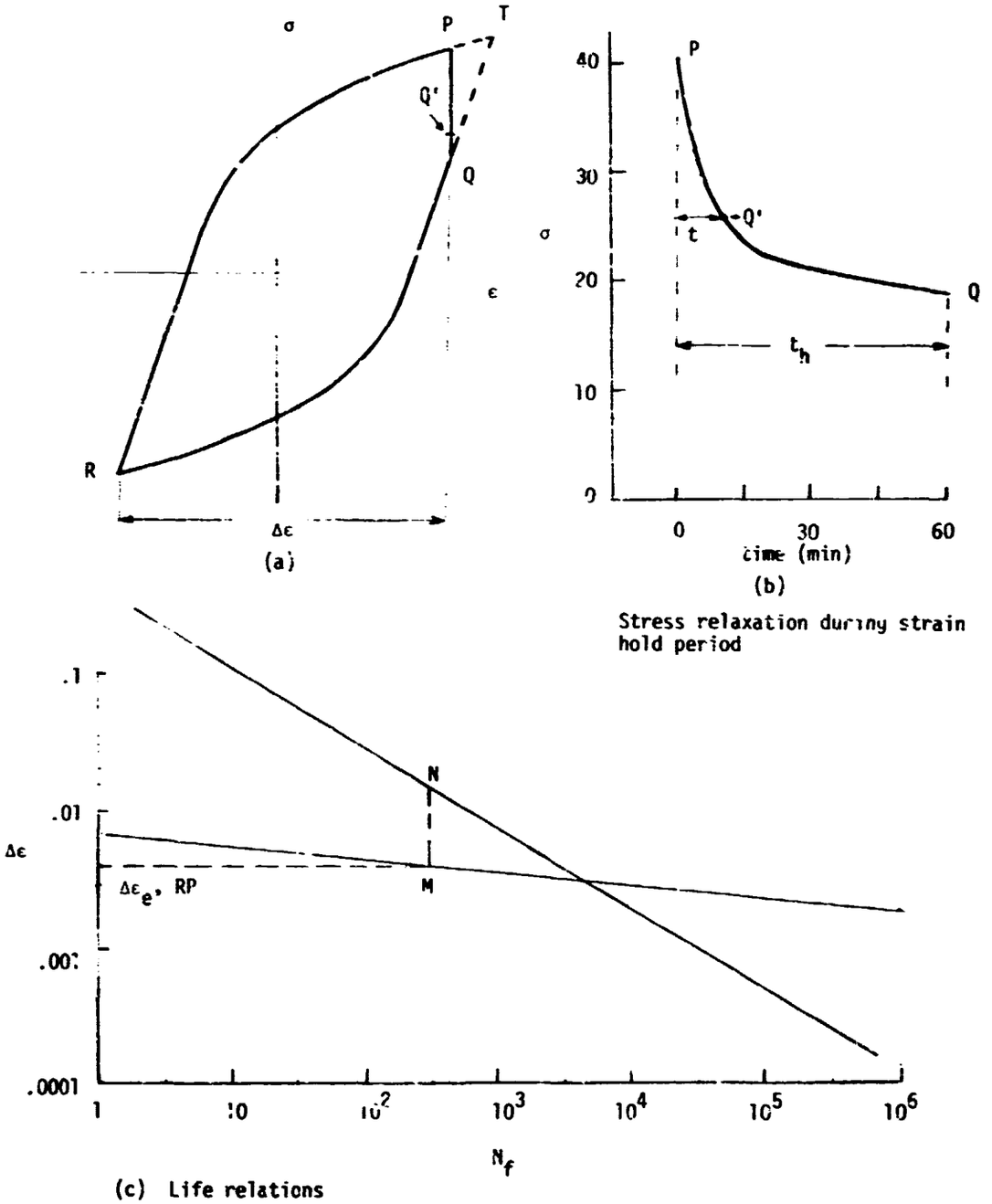

Stress relaxation during strain hold period

Fig. 4. Analysis of tensile-hold problem by engineering estimation of hysteresis loop.

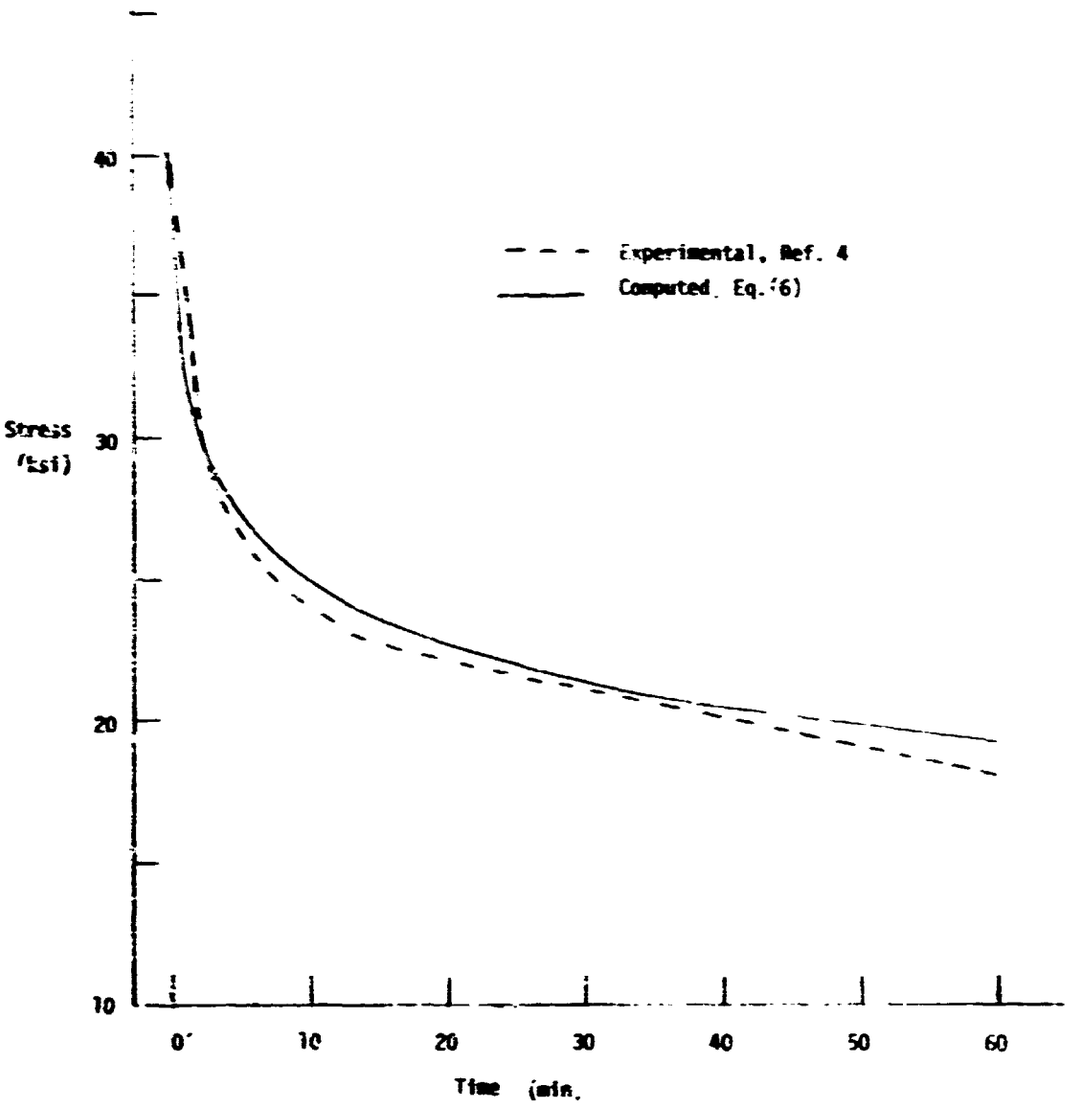

Fig. 5. Comparison with experimental observation of stress relaxation determined from power-law equation between stress and secondary creep rate.

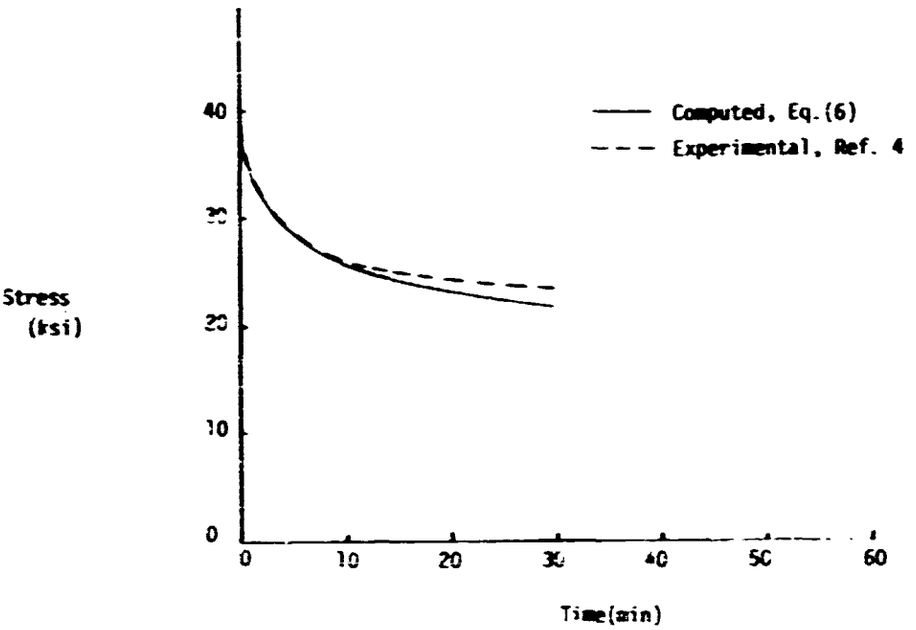
Computed, Eq.(6)
Experimental, Ref. 4
Stress
(ksi)
40
30
20
10
0
0
10
20
30
40
50
60
Time(min)

Fig. 5. (b)

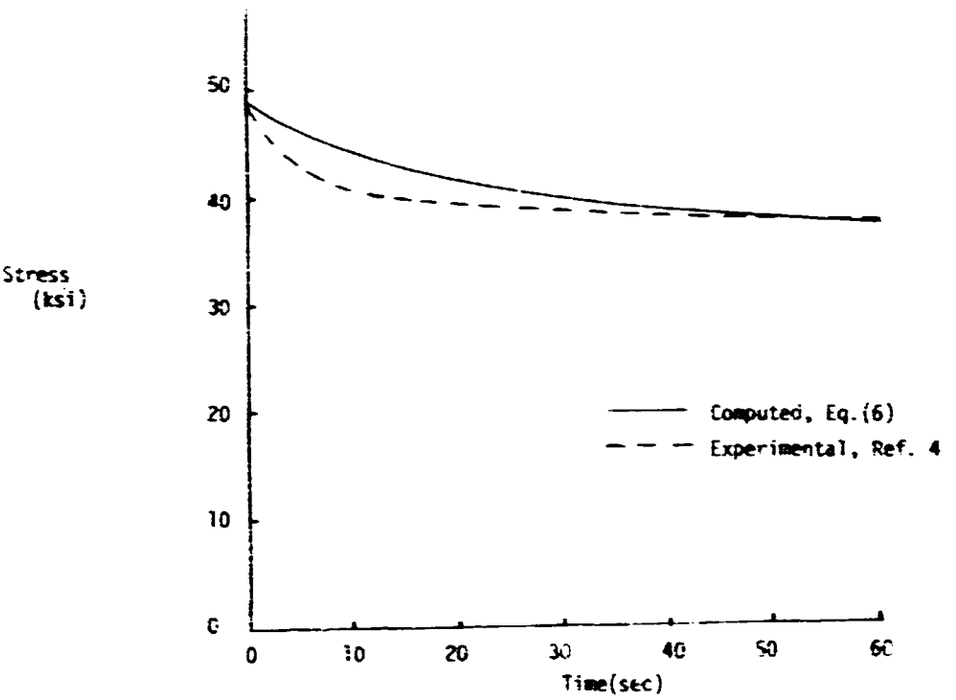
Stress
(ksi)
50
40
30
20
10
0
Computed, Eq.(6)
Experimental, Ref. 4
0
10
20
30
40
50
60
Time(sec)

Fig. 5. (c)

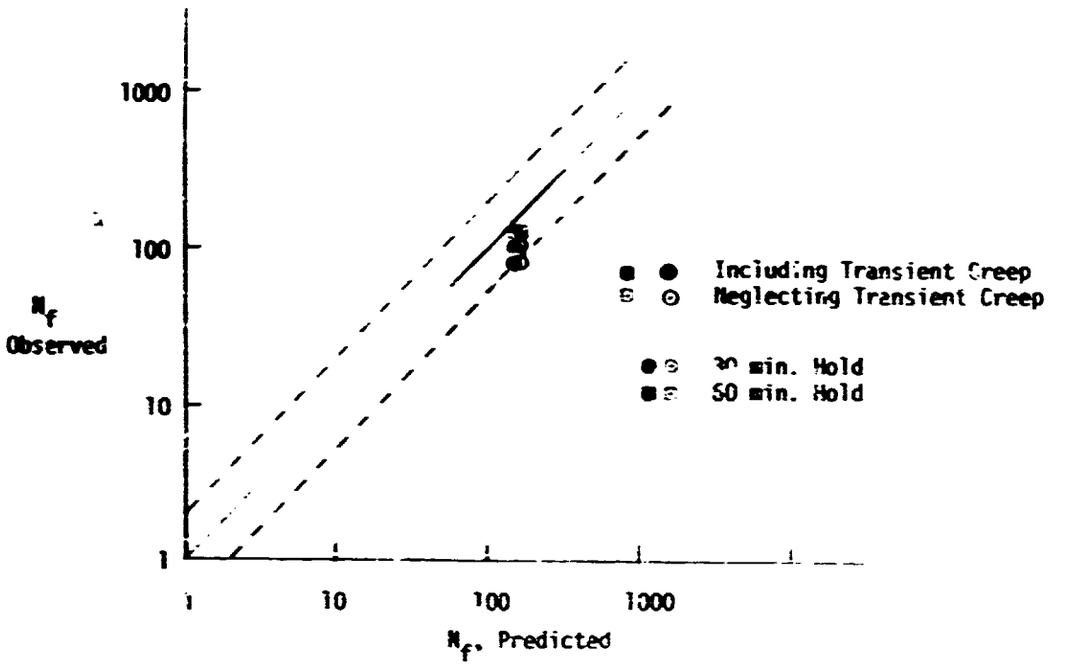

(a) Comparison of predicted and observed life values for high-strain tensile hold tests.

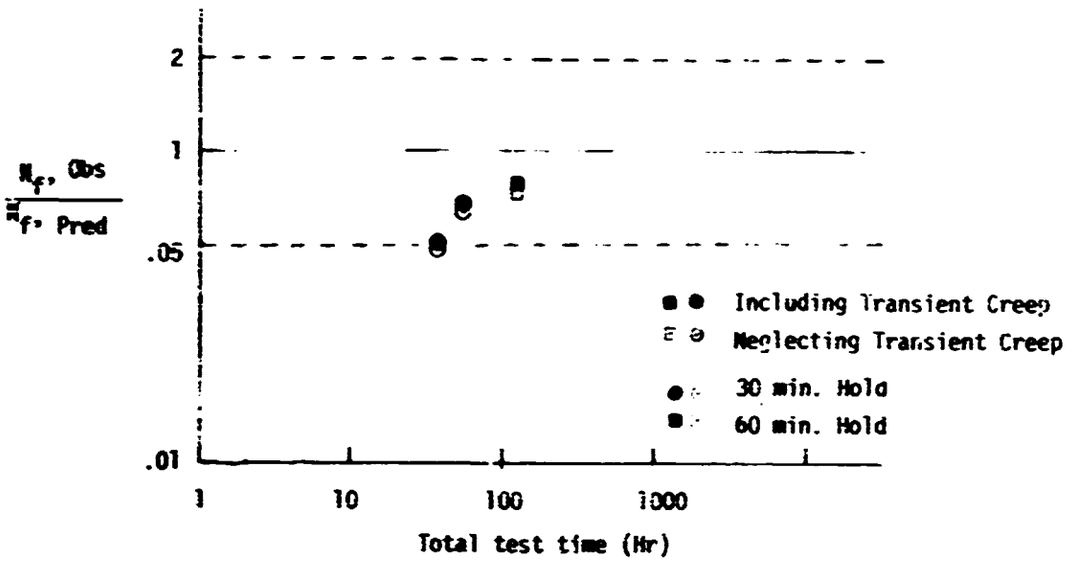

Fig. 6. Correlation of observed and predicted lives in tensile hold relaxation tests.

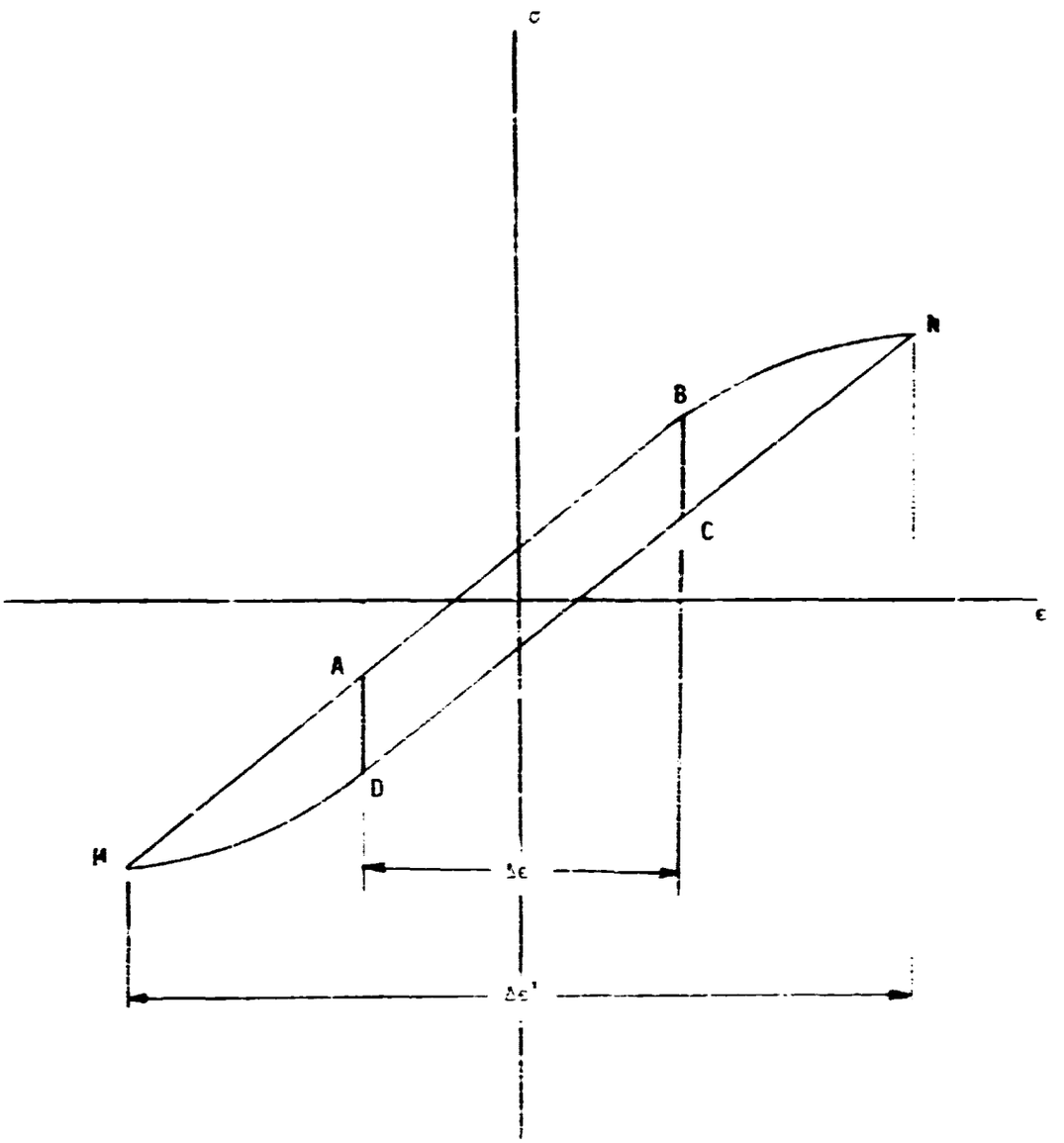

Fig. 7. Construction to simplify analyses of symmetrical hold tests.

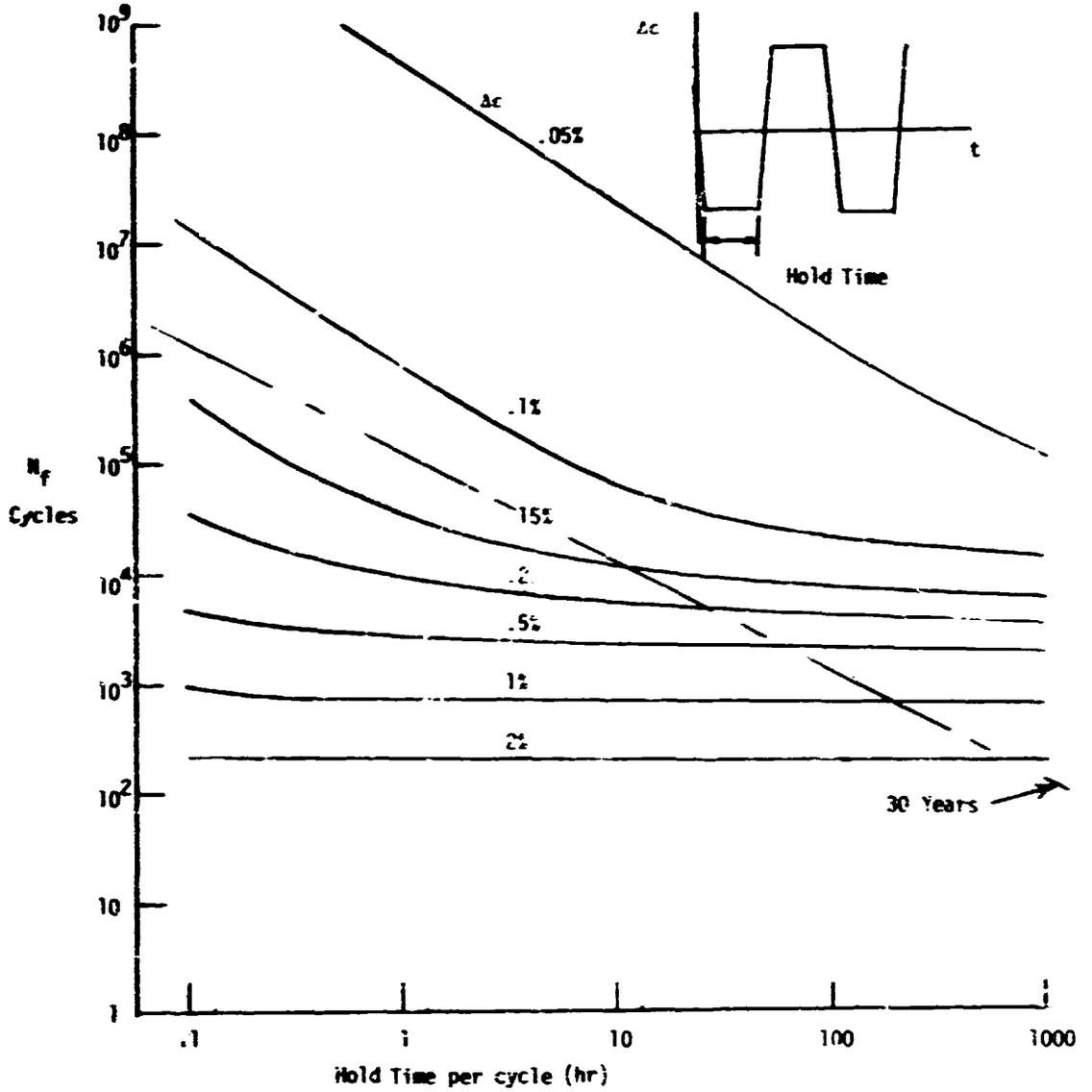

Fig. 8. Life relations for low strainranges and long hold-times with rapid strain ramping for 316 SS at 1300F, expressed with strainrange as parameter.

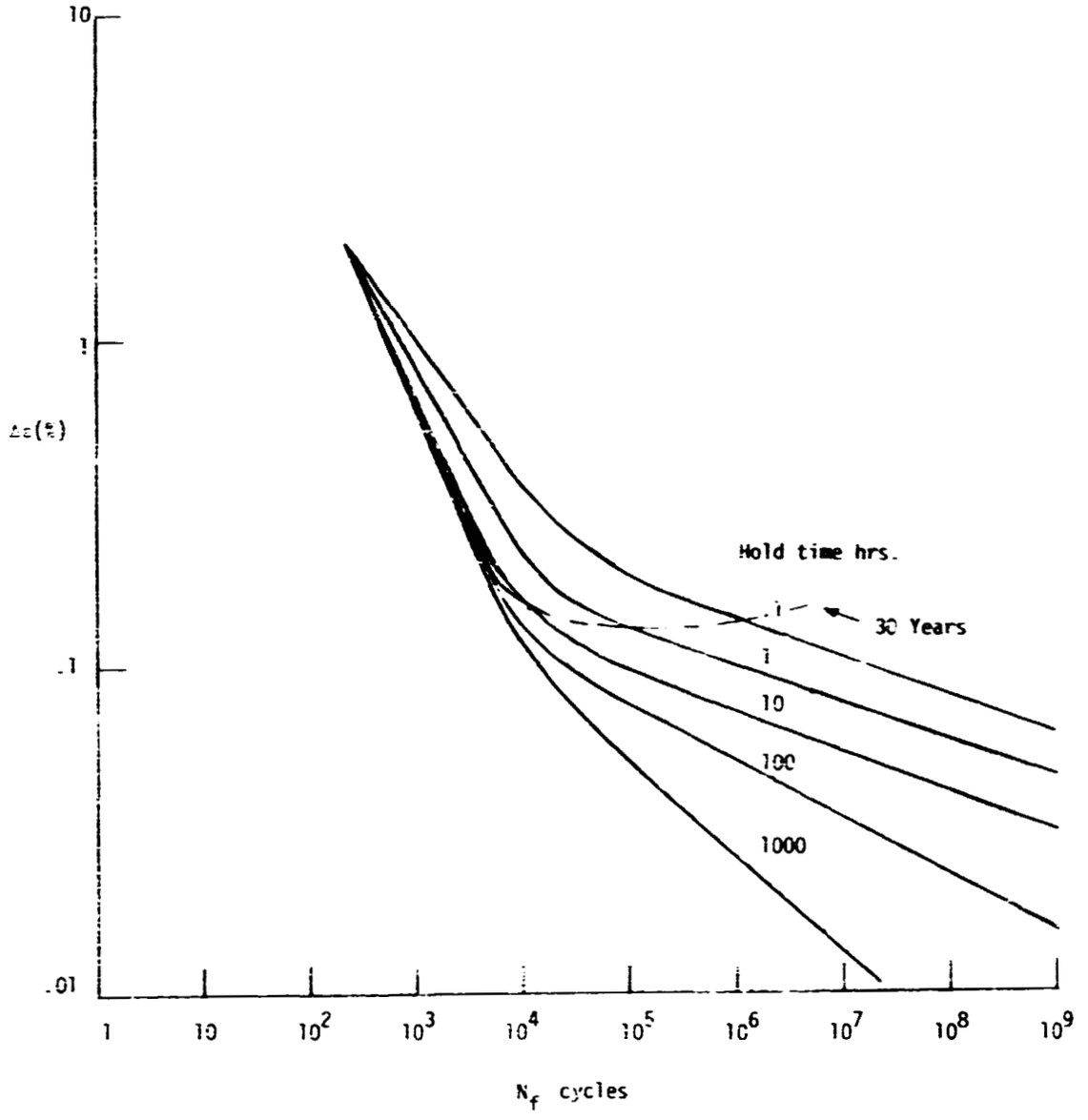

Fig. 9. Life relations for low strainranges and long hold times for 316 SS at 1300F expressed with hold time as parameter.

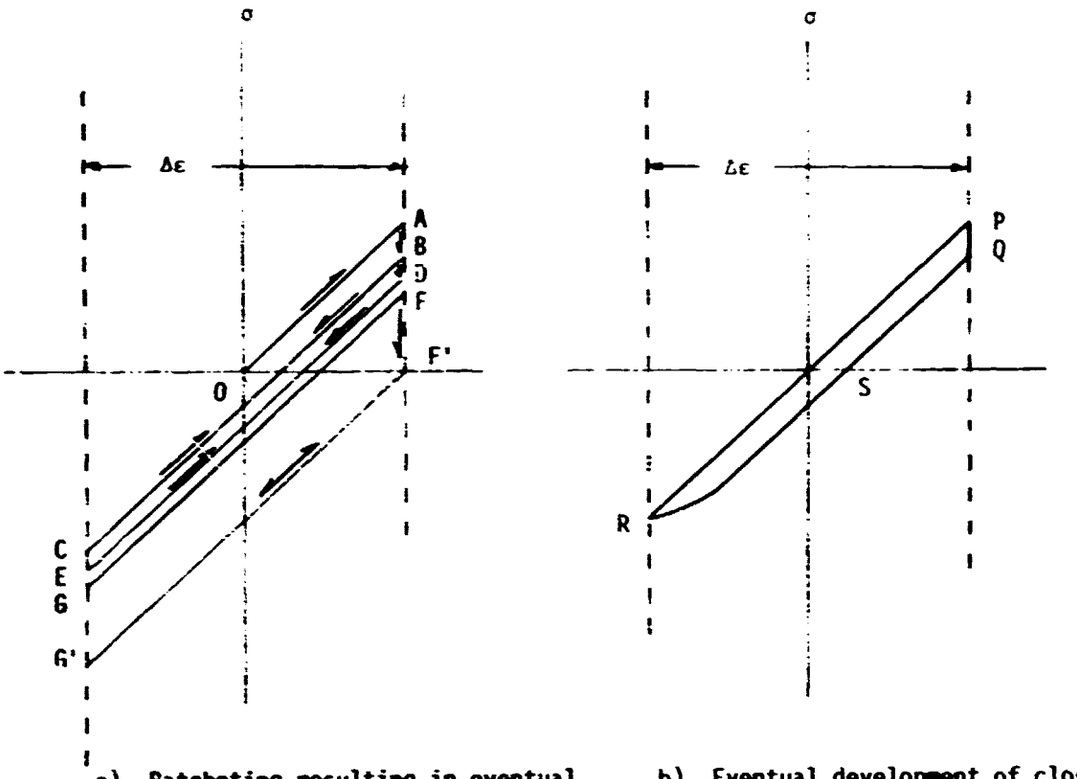

a) Ratcheting resulting in eventual shakedown wherein no cyclic inelastic strain develops.

b) Eventual development of closed hysteresis loop with cyclic inelastic strains.

Fig. 10. Two possible extremes of behavior in strain cycling at low strainrange with tensile hold periods.

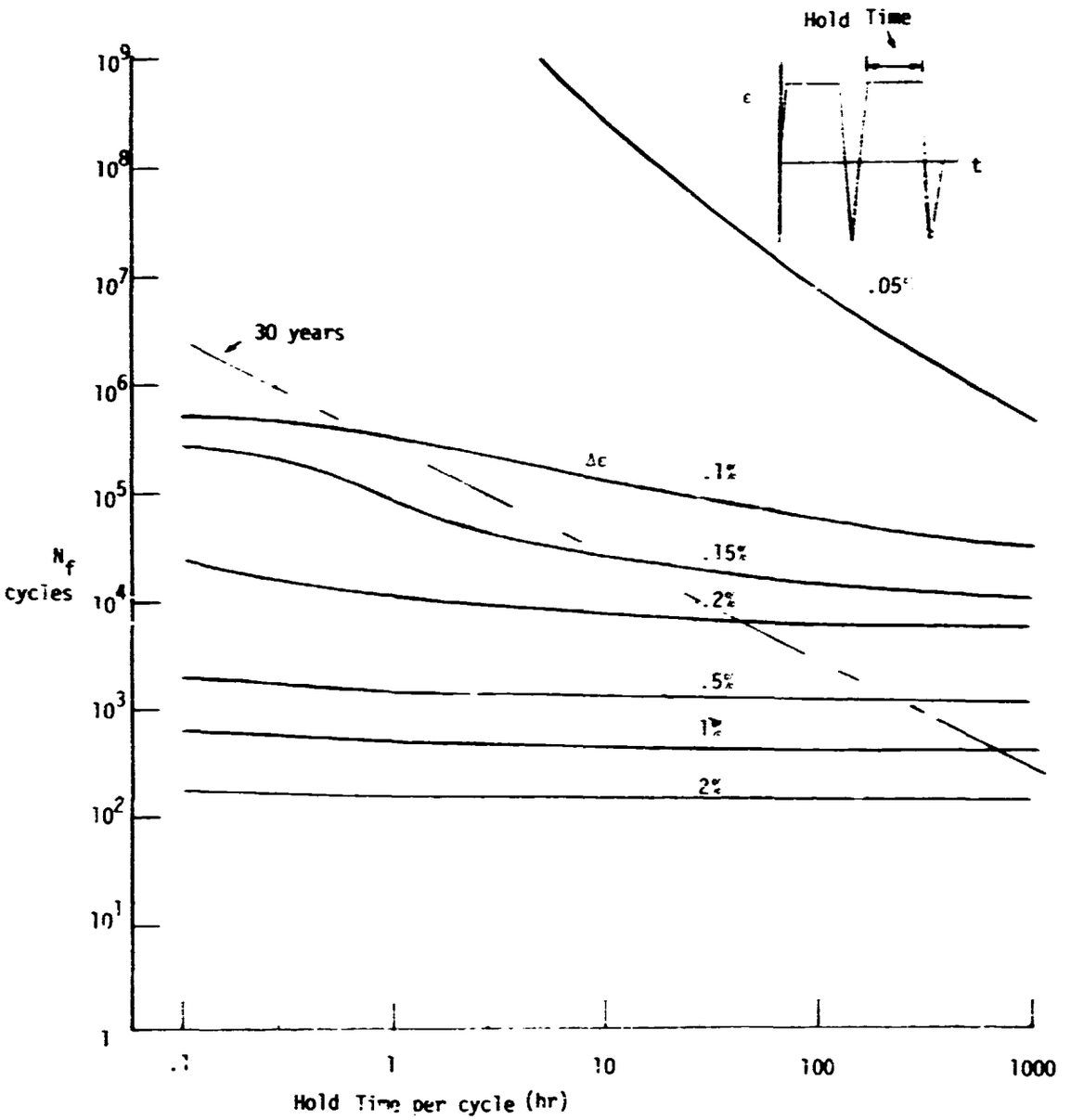

Fig. 11. Life relationships for low strainranges and long hold-times for rapid strain ramping combined with tensile hold at a maximum strain, 316 stainless steel at 1300F. Curves presented with strainrange as parameter.

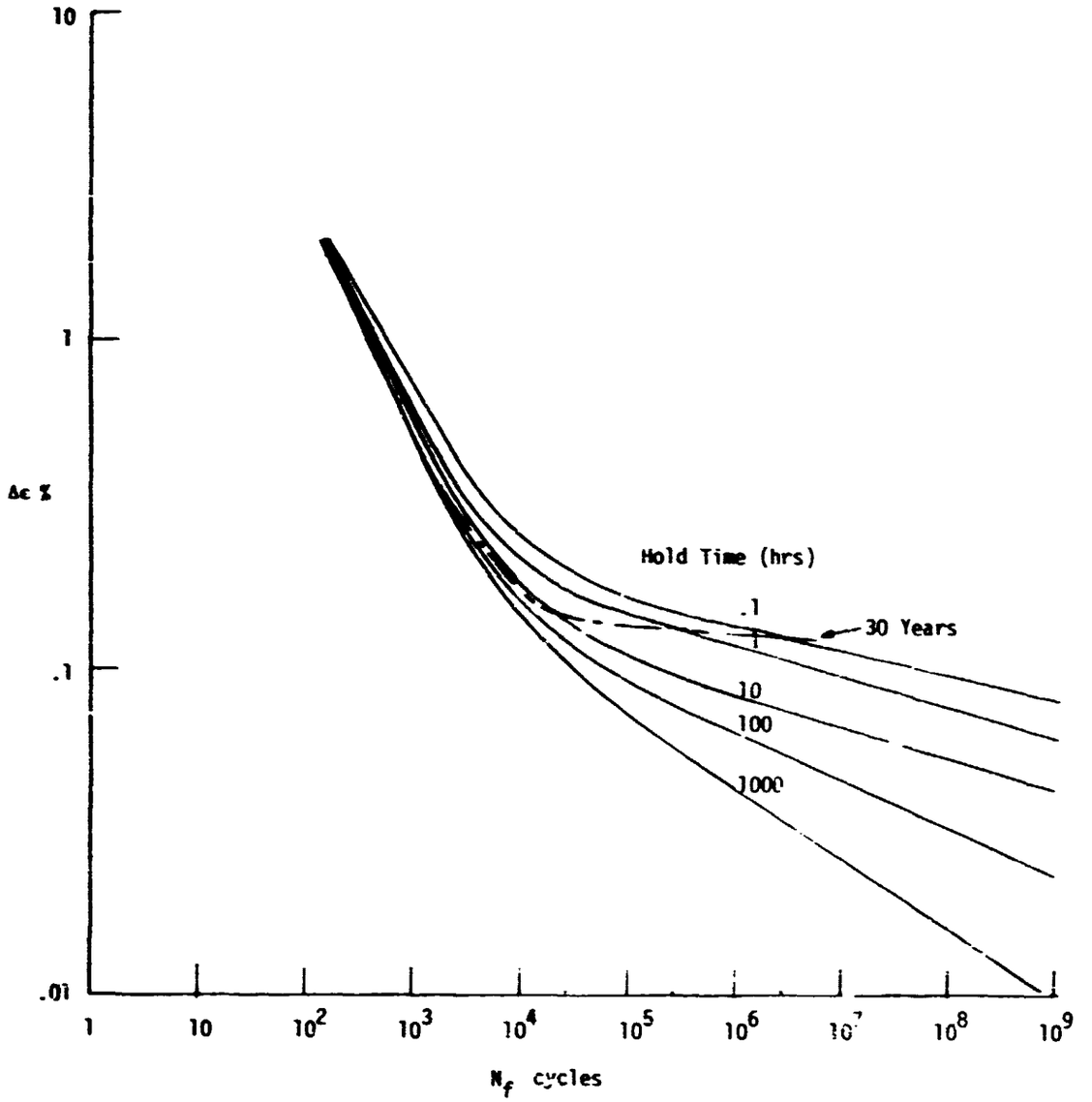

Fig. 12. Life relationships for low strainranges and long hold-times for rapid strain ramping combined with tensile hold at a maximum strain, 316 stainless steel at 1300F. Curves presented with hold time as parameter.

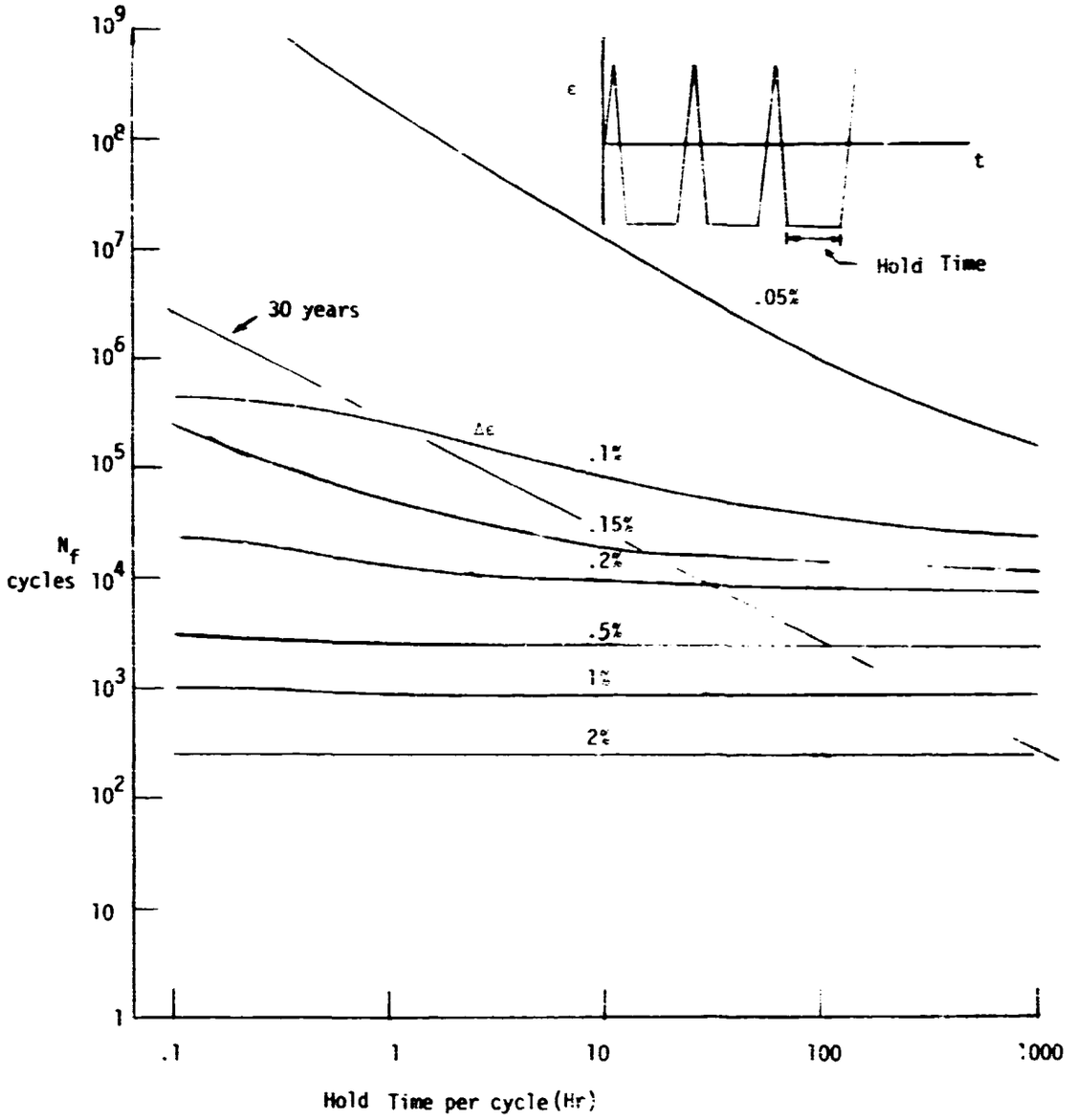

Fig. 13. Life relationships for low strainranges and long hold times for rapid strain ramping combined with compressive hold at maximum strain, 316 SS at 1300F.

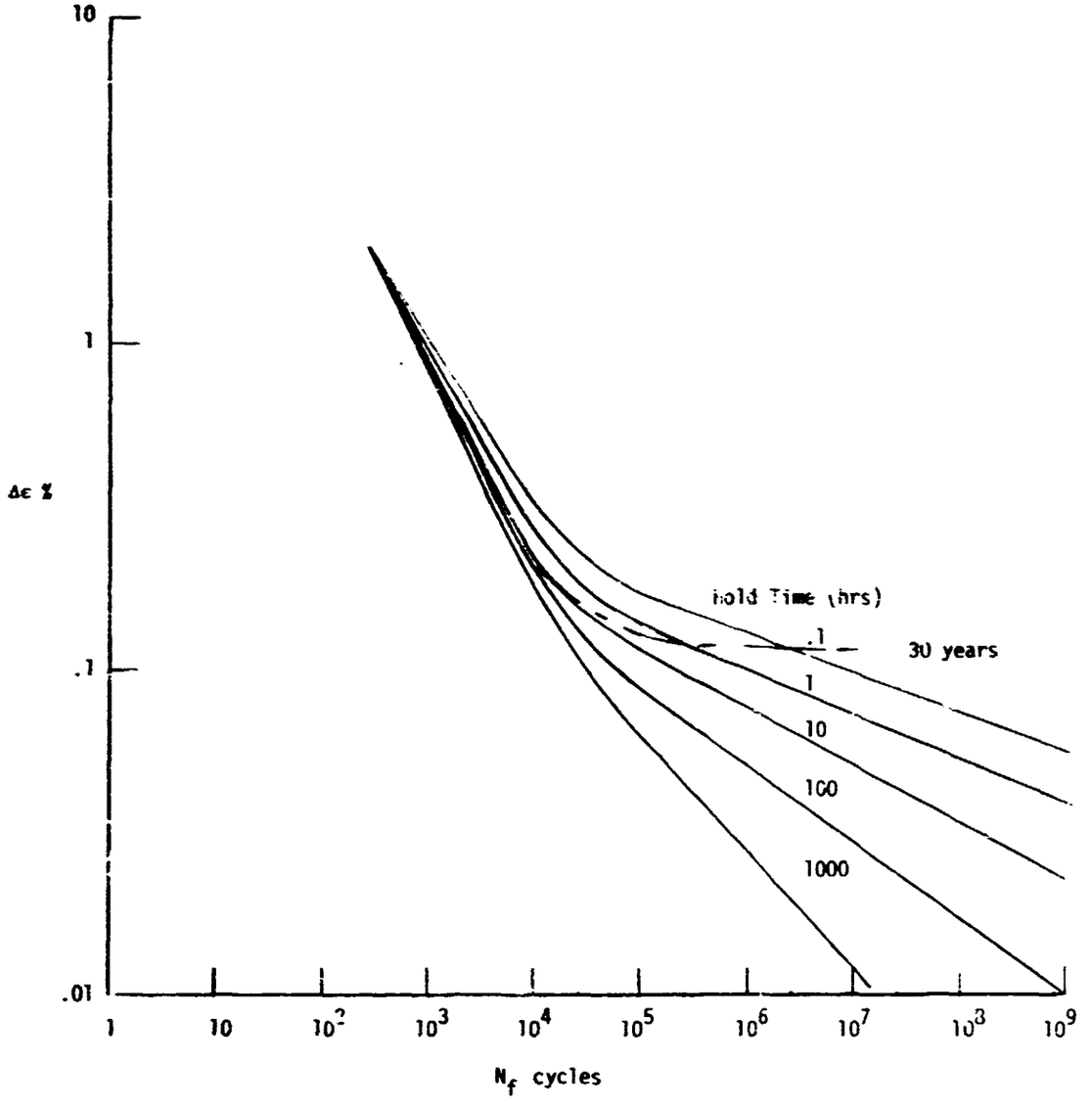

Fig. 14. Life relationships for low strainranges and long hold-times for rapid strain ramping combined with compressive hold at a maximum strain, 316 stainless steel at 1300F. Curves presented with hold-time as parameter.

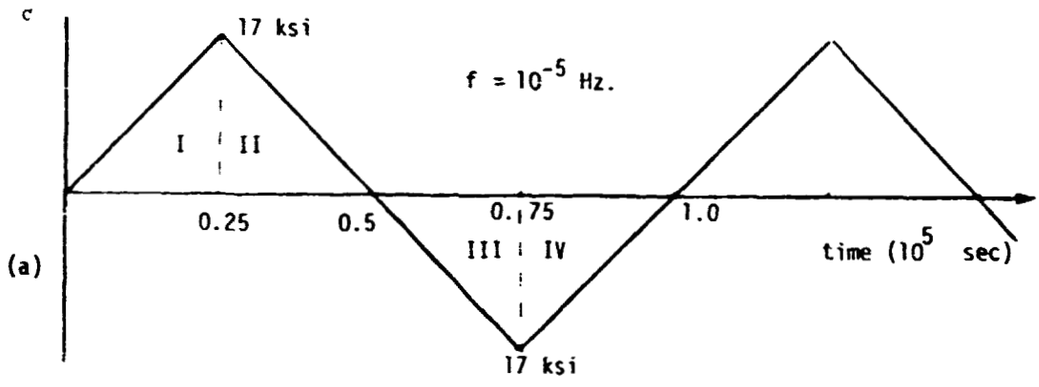

1. For quarter cycle I $\sigma = 6.8 \times 10^{-4} t$ t = sec., σ=ksi

$$\dot{\varepsilon}_c = 3.63 \times 10^{-16} \sigma^{7.14} = 8.791 \times 10^{-39} t^{7.14}.$$

$$\varepsilon_c = \int \dot{\varepsilon}_c \, dt = 8.791 \times 10^{-39} \int_0^{.25 \times 10^5} t^{7.14} \, dt = 6.802 \times 10^{-4}$$

For tensile half creep strain = $2 \times 6.802 \times 10^{-4} = 13.604 \times 10^{-4}$

2. Stress range = 34 ksi Elastic strainrange = $\frac{34}{20.5 \times 10^3} = 1.659 \times 10^{-3}$

3. From elastic and plastic life relations (or cyclic stress strain curve)

plastic strainrange for an elastic strainrange of 1.659×10^{-3} is 7.934×10^{-5}

4. $\Delta\varepsilon_{pp} = 7.934 \times 10^{-5}$, $\Delta\varepsilon_{cc} = 1.360 \times 10^{-3}$, $\Delta\varepsilon_{el} = 1.659 \times 10^{-3}$

5. $\Delta\varepsilon_t = \Delta\varepsilon_{pp} + \Delta\varepsilon_{cc} + \Delta\varepsilon_{el} = 3.098 \times 10^{-3}$

6. $f_{pp} = \frac{7.934 \times 10^{-5}}{7.934 \times 10^{-5} + 1.360 \times 10^{-3}} = .0551$

$f_{cc} = \frac{1.360 \times 10^{-3}}{7.934 \times 10^{-5} + 1.360 \times 10^{-3}} = .9449$

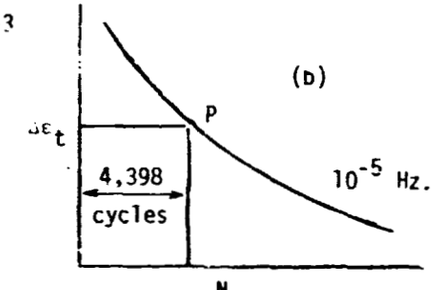

7. $\frac{1}{N_f} = \frac{f_{pp}}{N_{pp}} + \frac{f_{cc}}{N_{cc}} = \frac{.0551}{4.22 \times 10^3} + \frac{.9449}{1.60 \times 10^4}$

$N_f = 4{,}398$

$\Delta\varepsilon_t = 3.098 \times 10^{-3}$

$f = 10^{-5}$ Hz

Fig. 15. Illustrative computation for continuous stress ramping at low frequency and strainrange

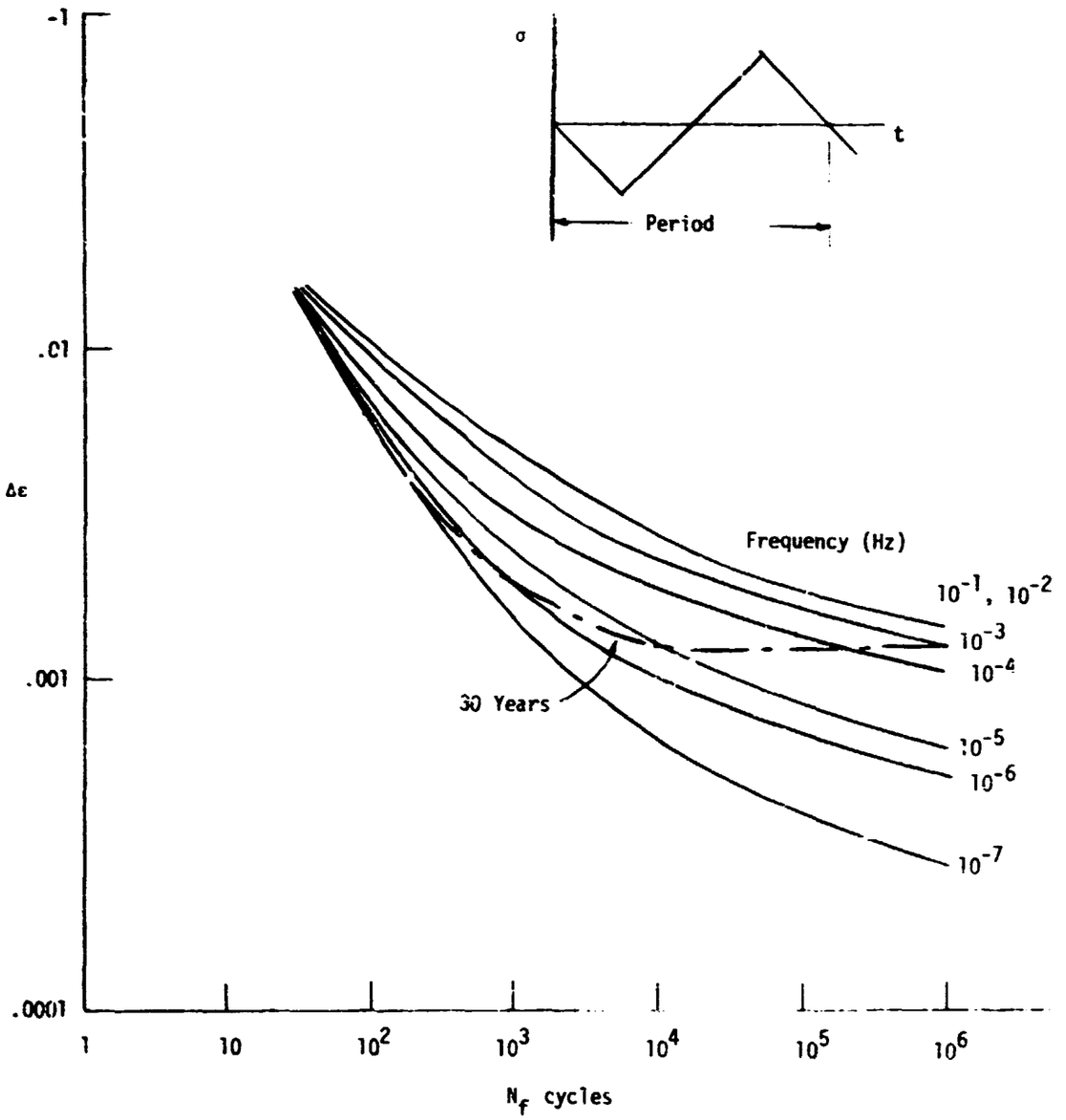

Fig. 16. Life relations in continuous stress ramping, of 316 SS, at 1300F, with frequency as a parameter.

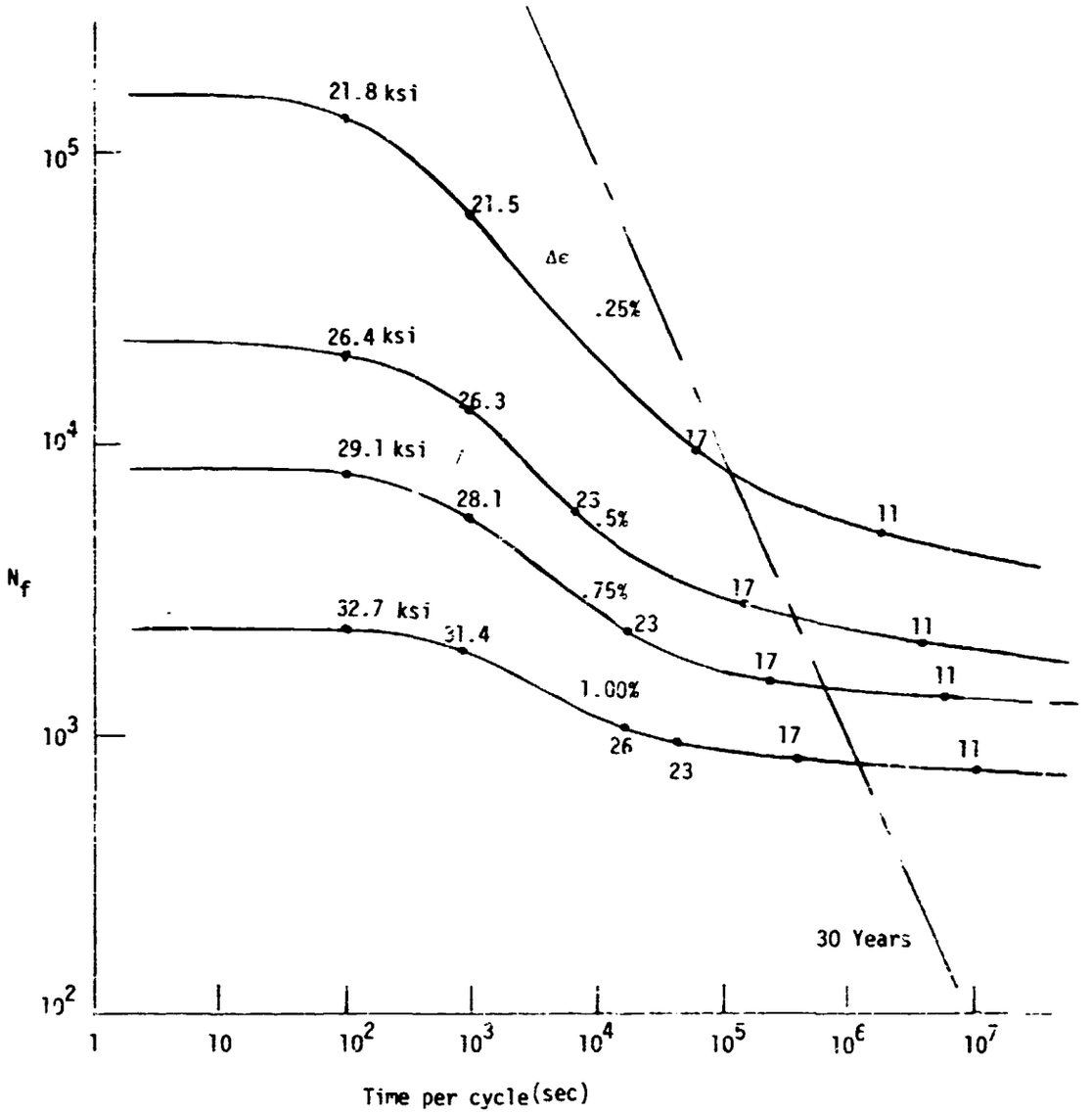

Fig. 17. Life Relations in continuous stress ramping, of 316 SS, at 1300F, with strainrange as a parameter.

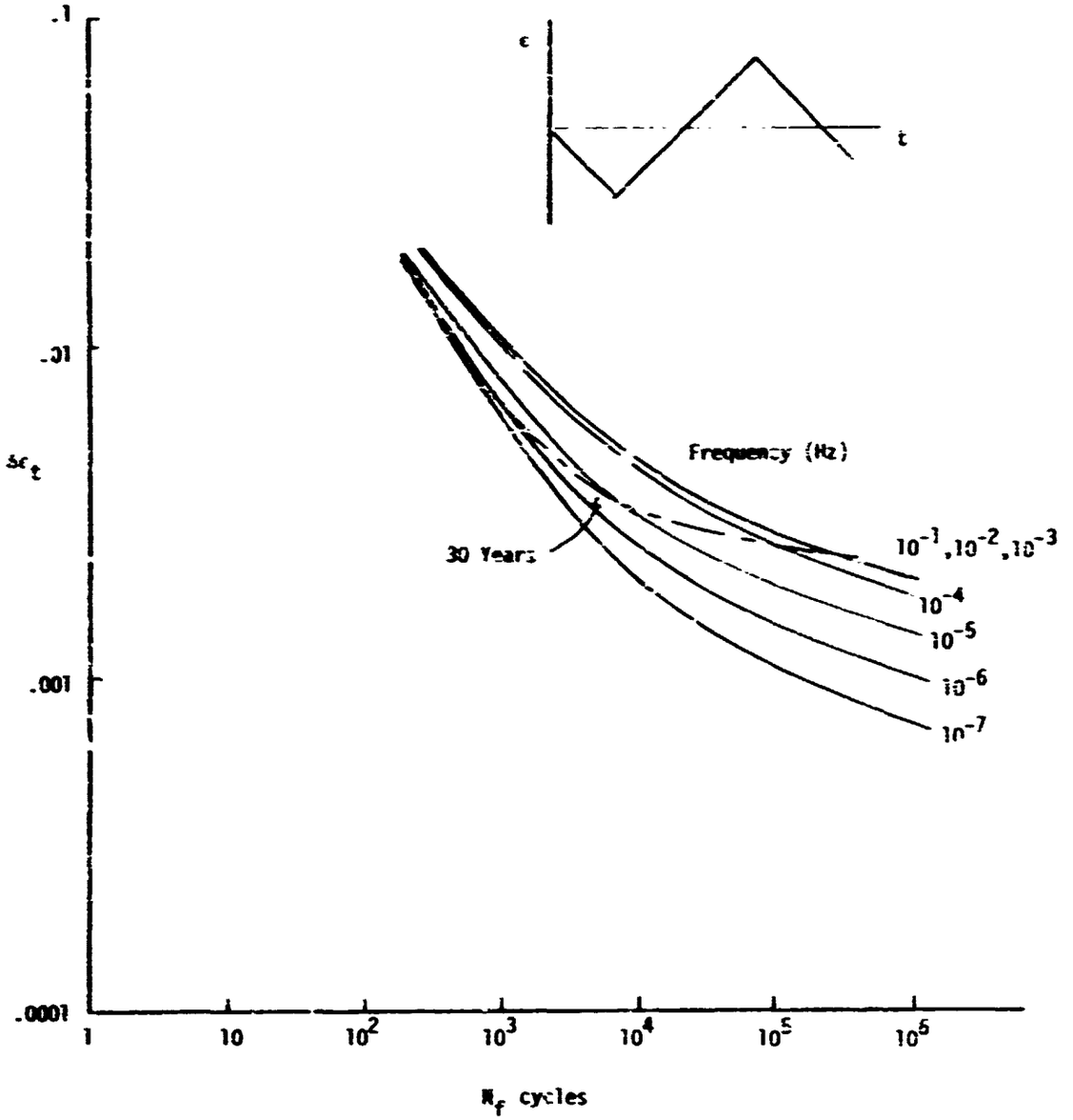

Fig. 18. Stress ramping, of 316 SS, at 1200F, with frequency as a parameter.

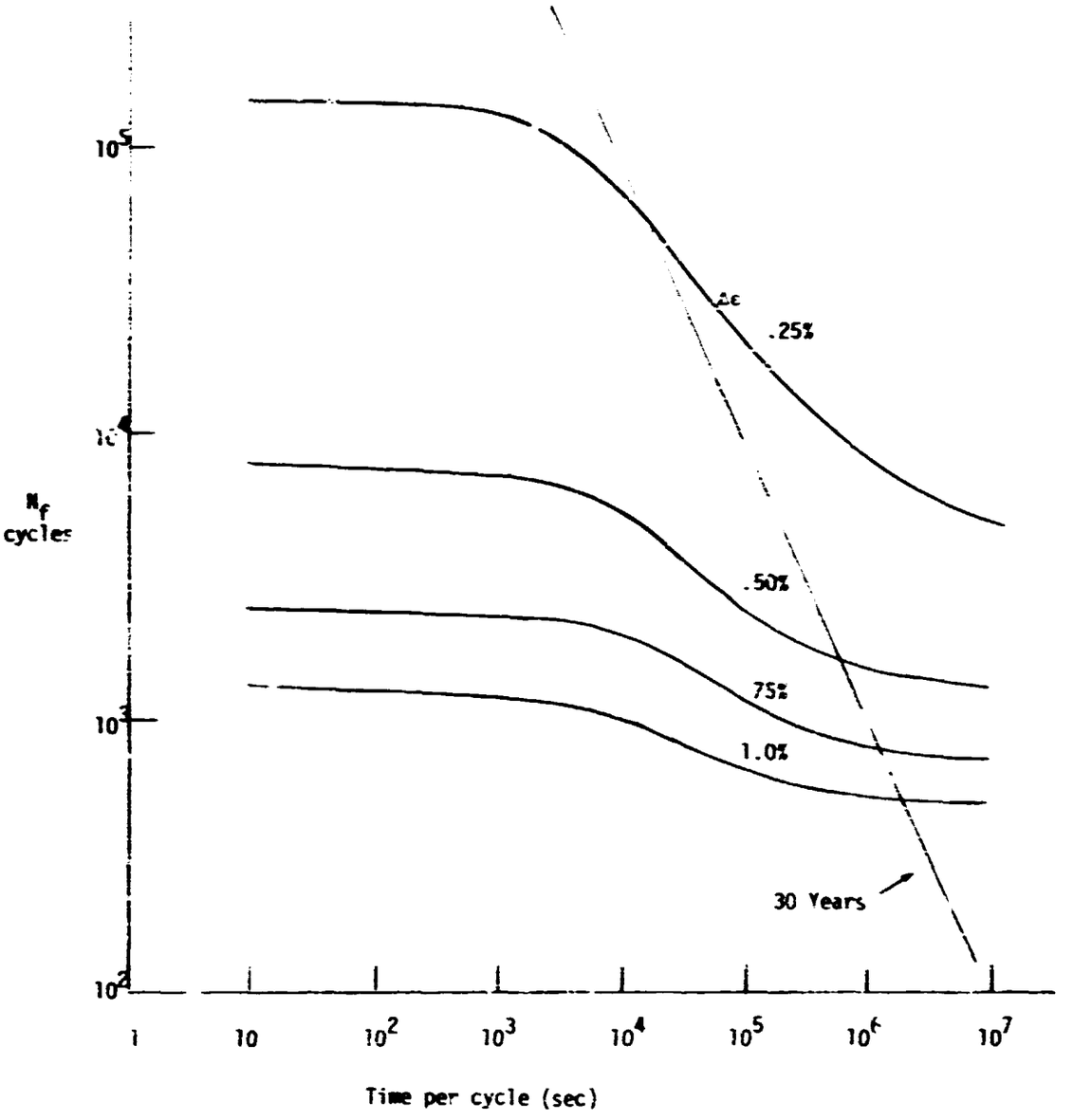

Fig. 19. Stress ramping, of 316 SS, at 1200F, with strainrange as a parameter.

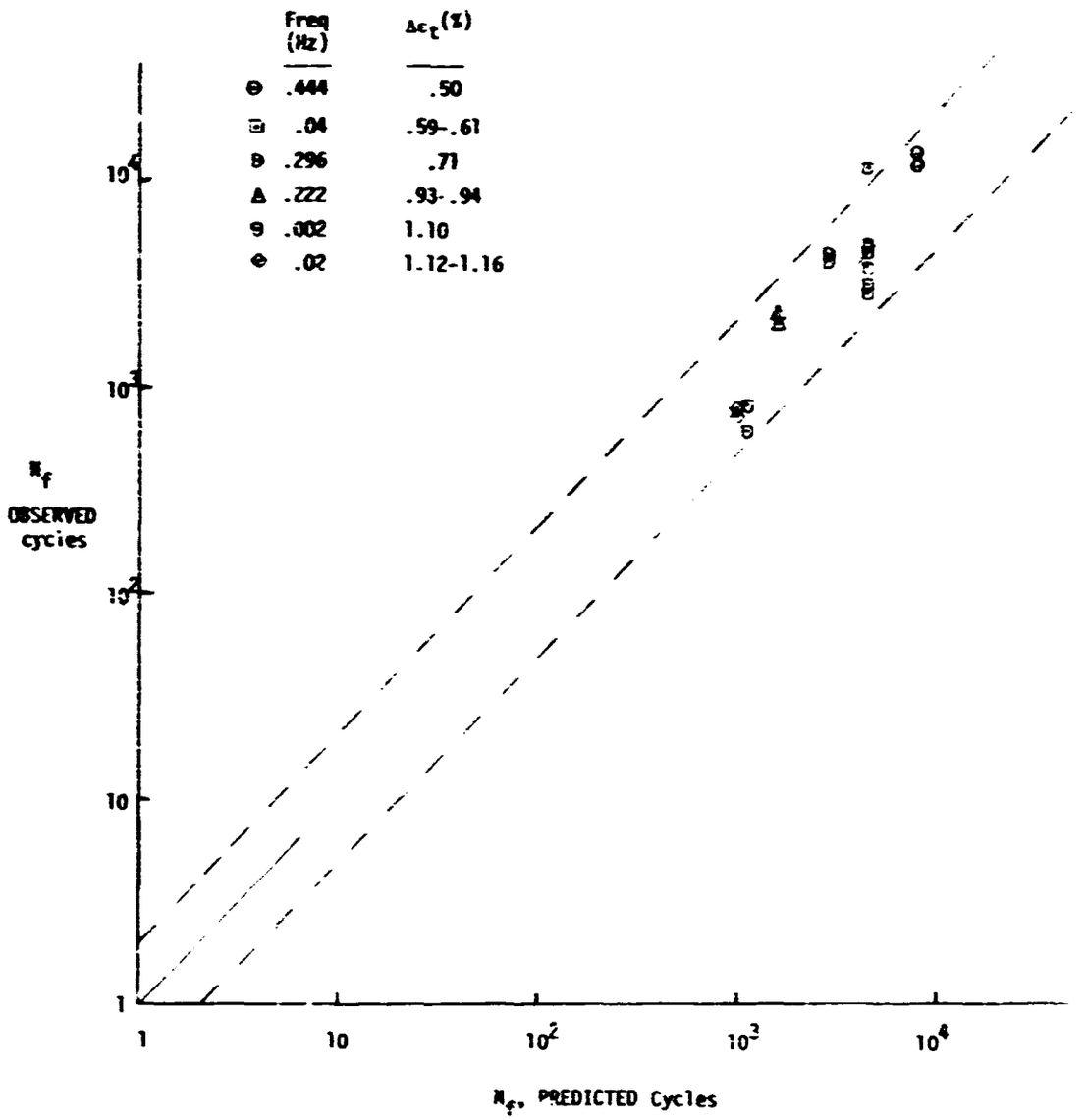

Fig. 20. Comparison of Predicted and Experimental life values for continuous strain cycling. Predictions made from continuous stress ramping calculations. Experiments determined from uniform strain ramping, of 316 SS, at 1200F.

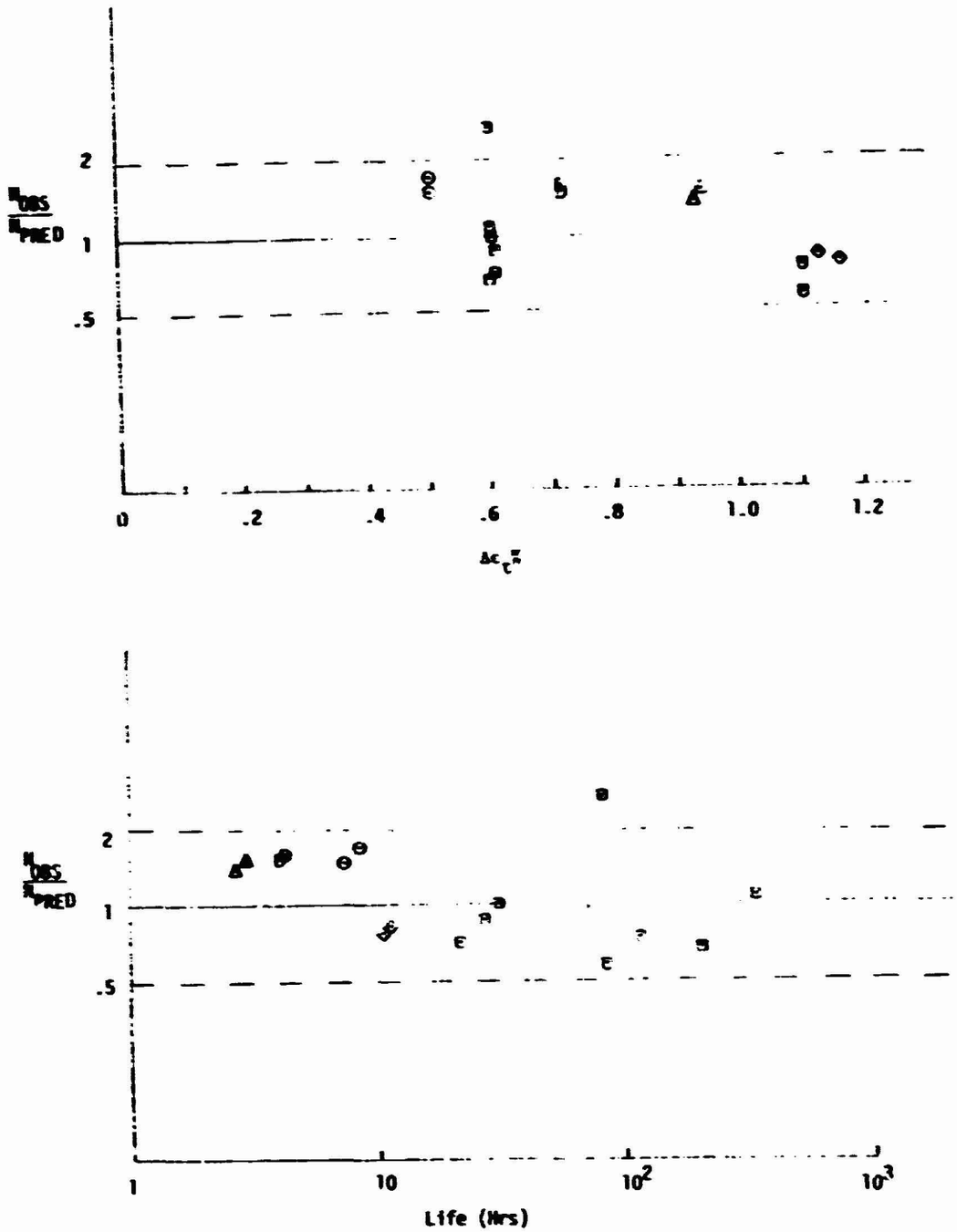
N_{OBS}/N_{PRED}
2
1
.5
0
.2
.4
.6
.8
1.0
1.2
Δc_{ζ}^{m}
N_{OBS}/N_{PRED}
2
1
.5
1
10
10^2
10^3
Life (Hrs)

Fig. 20 (cont.)

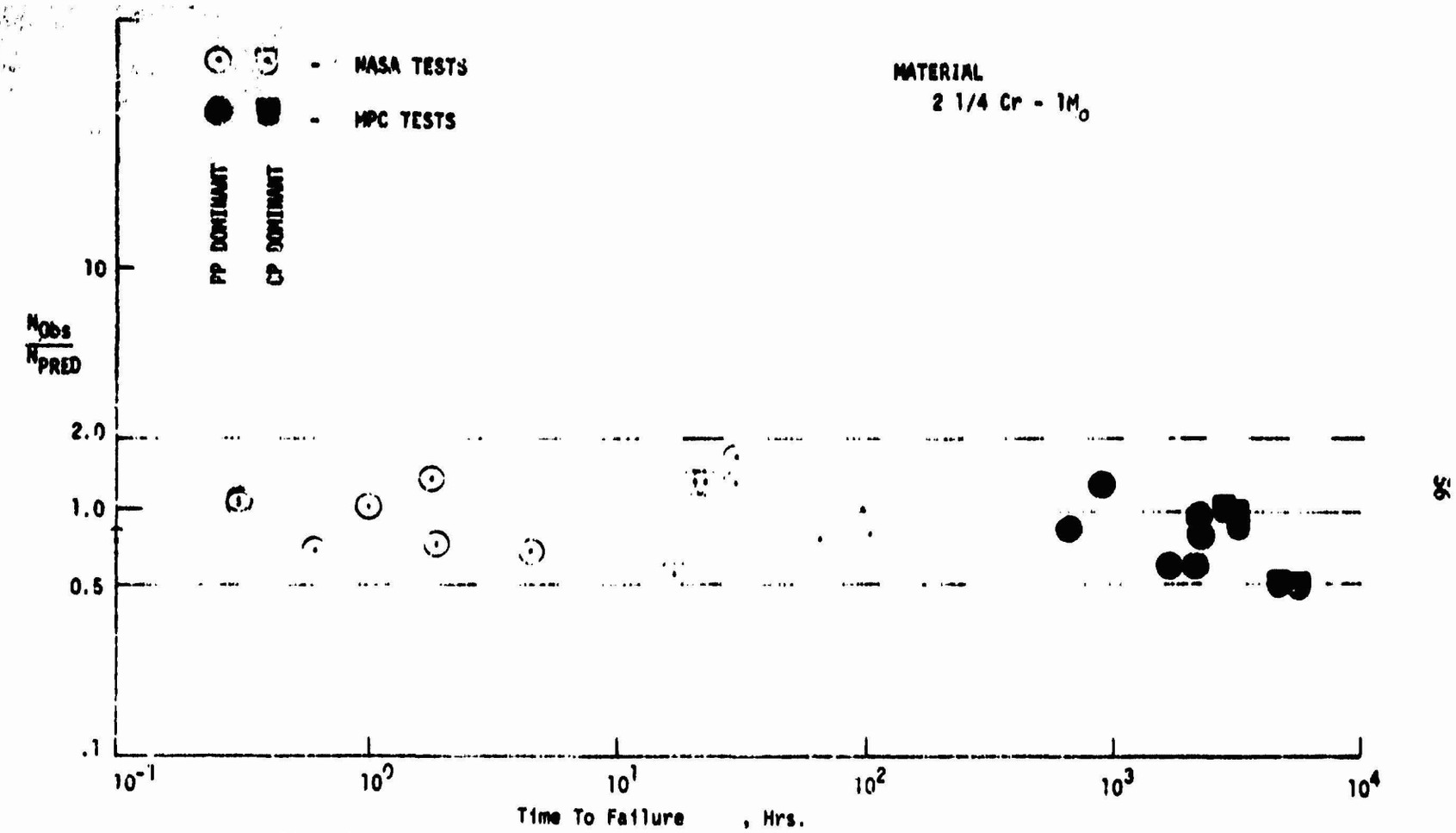

Fig. 21. Correlation of observed and predicted lines over a large spectrum of failure times for 2 1/4 Cr-1 Mo Steel at 900-1100 F.

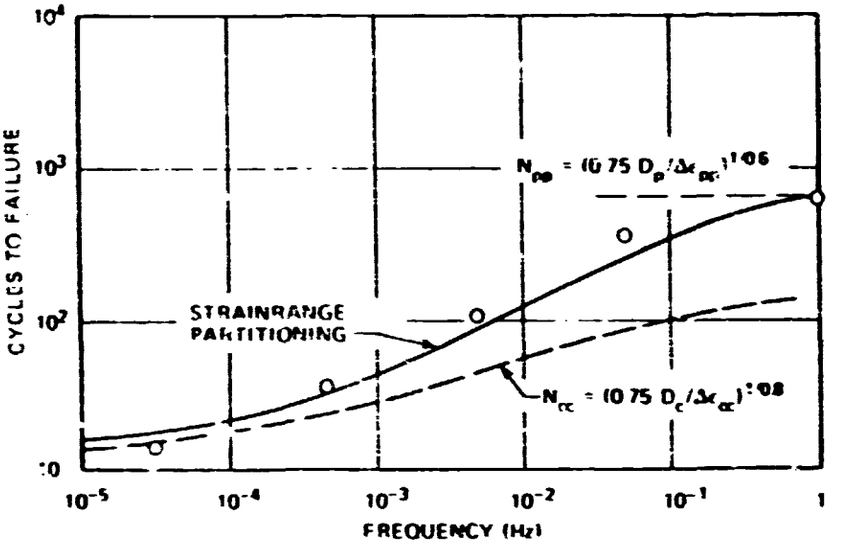

Fig. 22. Application of Strainrange Partitioning to study of frequency effect for a material with time-dependent creep ductility; A-286 tested at 1100°F (595°C), $\Delta\epsilon_{in} = 0.009$.

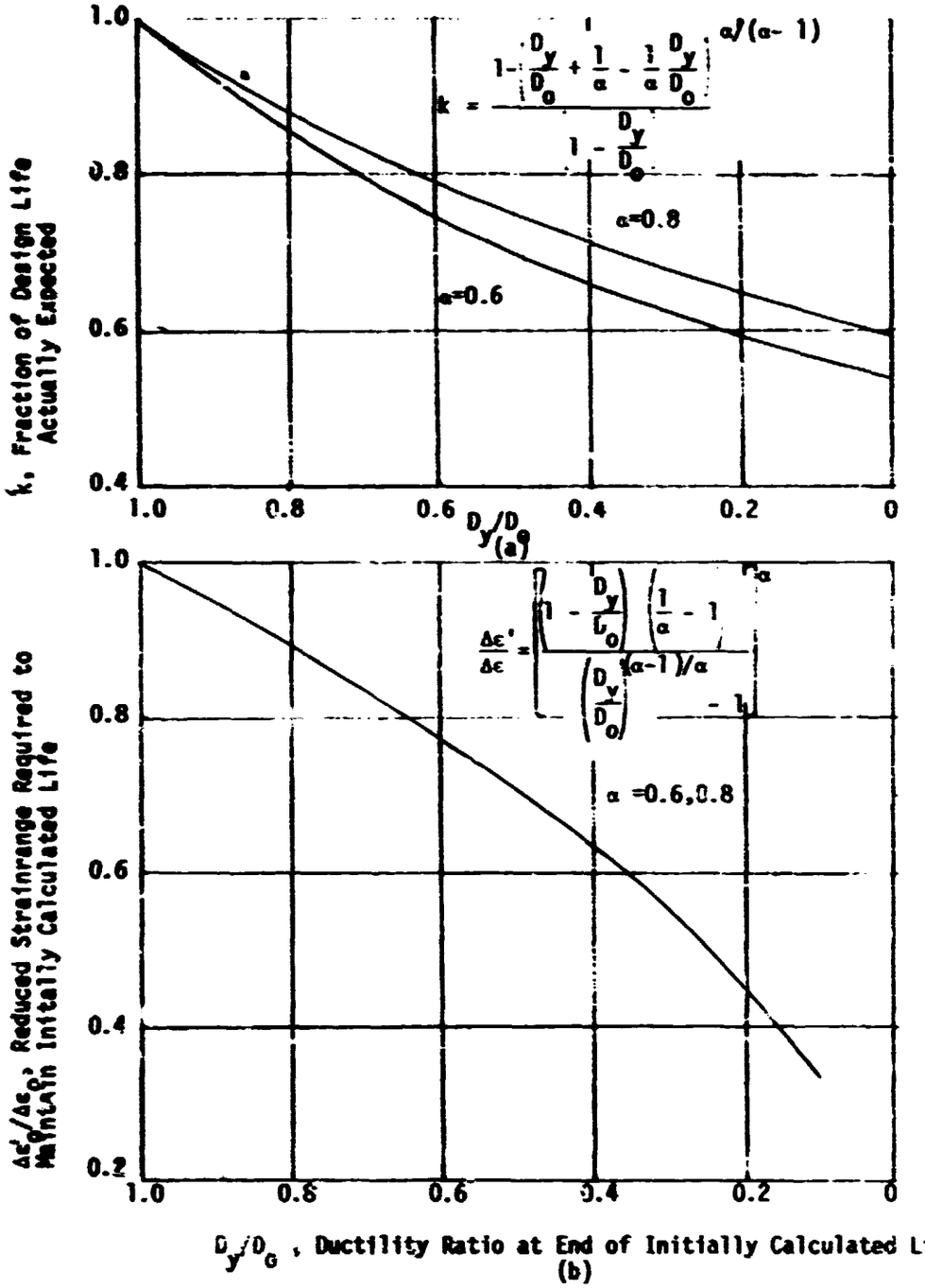

Fig. 23. Application of Strainrange Partitioning to estimate embrittling effects. (a) Strainrange maintained constant, life reduced; (b) Strainrange reduced to restore life to initially calculated value.

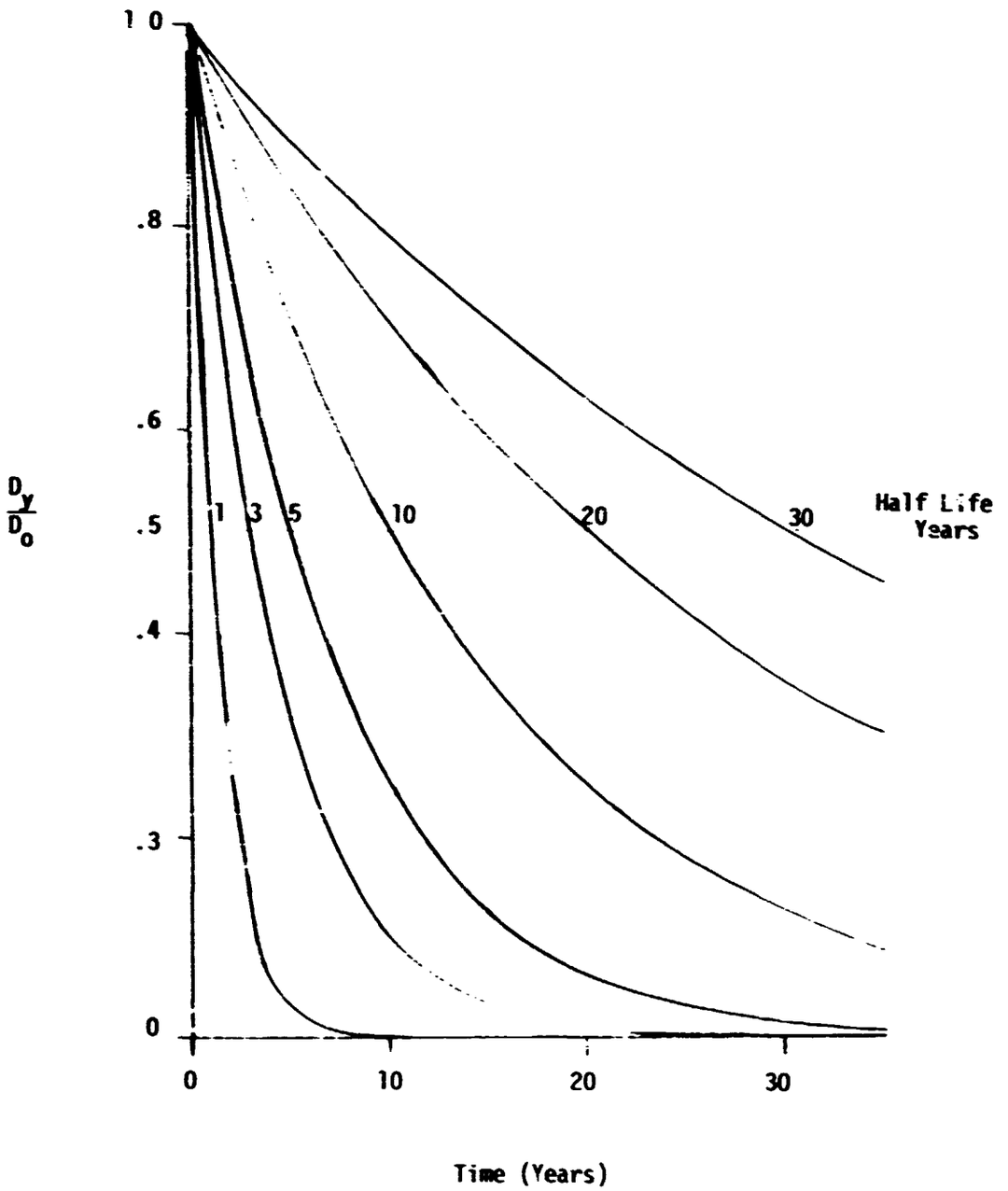

Fig. 24. Hypothesized ductility variations for use in life calculations

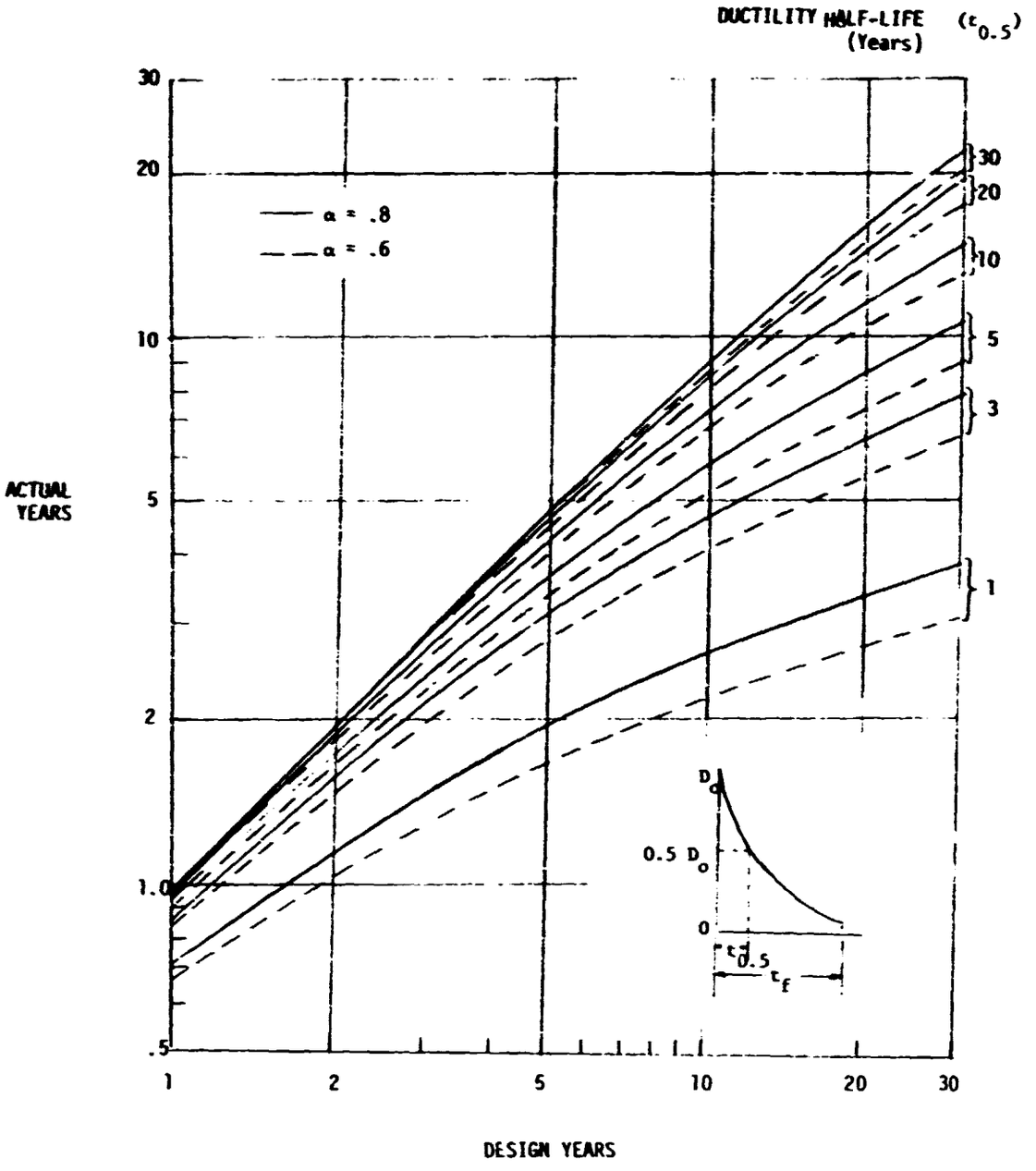

Fig. 25 Calculated fatigue life for exponential decay of ductility.